

Diverse mitotic functions of the cytoskeletal cross-linking protein Shortstop suggest a role in Dynein/Dynactin activity

Evan B. Dewey and Christopher A. Johnston*

Department of Biology, University of New Mexico, Albuquerque, NM 87131

ABSTRACT Proper assembly and orientation of the bipolar mitotic spindle is critical to the fidelity of cell division. Mitotic precision fundamentally contributes to cell fate specification, tissue development and homeostasis, and chromosome distribution within daughter cells. Defects in these events are thought to contribute to several human diseases. The underlying mechanisms that function in spindle morphogenesis and positioning remain incompletely defined, however. Here we describe diverse roles for the actin-microtubule cross-linker Shortstop (Shot) in mitotic spindle function in *Drosophila*. Shot localizes to mitotic spindle poles, and its knockdown results in an unfocused spindle pole morphology and a disruption of proper spindle orientation. Loss of Shot also leads to chromosome congression defects, cell cycle progression delay, and defective chromosome segregation during anaphase. These mitotic errors trigger apoptosis in *Drosophila* epithelial tissue, and blocking this apoptotic response results in a marked induction of the epithelial–mesenchymal transition marker MMP-1. The actin-binding domain of Shot directly interacts with Actin-related protein-1 (Arp-1), a key component of the Dynein/Dynactin complex. Knockdown of Arp-1 phenocopies Shot loss universally, whereas chemical disruption of F-actin does so selectively. Our work highlights novel roles for Shot in mitosis and suggests a mechanism involving Dynein/Dynactin activation.

Monitoring Editor

Yukiko Yamashita
University of Michigan

Received: Apr 6, 2017

Revised: Jun 19, 2017

Accepted: Jul 19, 2017

INTRODUCTION

The cytoskeleton, consisting of microtubules (MTs), intermediate filaments, and filamentous actin filaments (F-actin), vitally contributes to diverse cellular processes, including signal transduction,

intracellular transport, chromosome segregation, and cytokinesis (Fletcher and Mullins, 2010). MTs and F-actin each undergo dynamic assembly and disassembly processes, both during interphase and throughout cell division. Coordination between the actin cytoskeleton and MTs is important for the establishment of cell polarity, where movement along microtubules promotes cortical localization of polarity cues that are subsequently stabilized by the cortical F-actin network (Li and Gundersen, 2008). During mitosis, actin and MTs cooperatively orchestrate several important cell shape changes necessary for division. For example, central spindle MTs promote Rho activation at the cell equator necessary for polymerization of the F-actin dense cytokinetic ring (Ramkumar and Baum, 2016). In turn, cortical actin plays an important role in mitotic spindle assembly and orientation in many systems (Sandquist *et al.*, 2011). Thus F-actin and MTs can be considered partners in regulating key cellular processes.

To aid in their coordination, several protein families can provide direct physical interactions between cytoskeletal components that stabilize their structural integrities and generate dynamic forces (Huber *et al.*, 2015). Spectraplakins, members of the spectrin protein superfamily, are an evolutionarily conserved class of cytoskeletal cross-linking proteins (Suoizzi *et al.*, 2012). These large proteins

This article was published online ahead of print in MBoC in Press (<http://www.molbiolcell.org/cgi/doi/10.1091/mbc.E17-04-0219>) on July 26, 2017.

*Address correspondence to: Christopher A. Johnston (johnstca@unm.edu).

Abbreviations used: ABD, actin-binding domain; ACF7, actin cross-linking factor 7; Arp-1, actin-related protein-1; BSA, bovine serum albumin; CH, calponin homology; CID, centromere Identifier; C-MT, centrosomal MT; Cyt-D, cytochalasin-D; Dhc, Dynein heavy-chain; DMSO, dimethyl sulfoxide; DTT, dithiothreitol; EMT, epithelial–mesenchymal transition; ERM, Ezrin–Radixin–Moesin; F-actin, filamentous actin; Fz/Dsh, Frizzled/Dishevelled; GAS2, Growth Arrest Specific Protein 2; GFP, green fluorescent protein; GST, glutathione S-transferase; IPTG, isopropyl β -D-1-thiogalactopyranoside; MACF1, microtubule actin cross-linking factor 1; MBD, MT-binding domain; MMP-1, Matrix metalloproteinase 1; MT, microtubule; NEB, nuclear envelope breakdown; PBS, phosphate-buffered saline; PEFs, polar ejection forces; PH, pleckstrin homology; PH3, phosphohistone-H3; RNAi, RNA interference; SAC, spindle assembly checkpoint; Shot, Shortstop; UTR, untranslated region.

© 2017 Dewey and Johnston. This article is distributed by The American Society for Cell Biology under license from the author(s). Two months after publication it is available to the public under an Attribution–Noncommercial–Share Alike 3.0 Unported Creative Commons License (<http://creativecommons.org/licenses/by-nc-sa/3.0>).

“ASCB®,” “The American Society for Cell Biology®,” and “Molecular Biology of the Cell®” are registered trademarks of The American Society for Cell Biology.

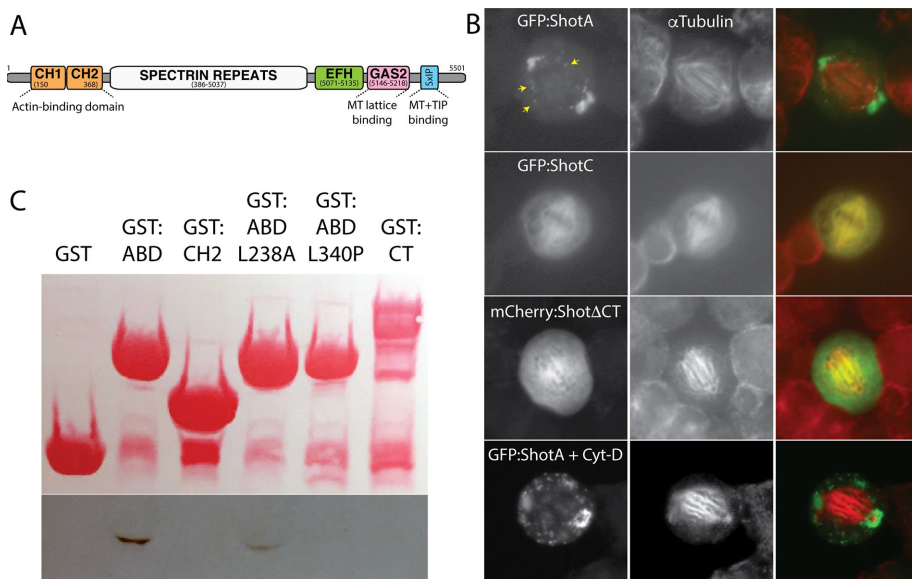


FIGURE 1: Shot localizes to mitotic spindle poles and directly binds Arp-1. (A) Domain diagram illustrates the modular structure of Shot. Tandem CH domains bind F-actin filaments; Spectrin repeats provide the core central structure; EF Hand (EFH) domain has no described function; Growth arrest specific protein 2 (GAS2) domain binds microtubule lattices; SxIP motif binds EB1 for microtubule +TIP localization. (B) Full-length ShotA localizes primarily to mitotic poles, with additional puncta found along spindle microtubules (yellow arrows). ShotC, lacking the CH1 domain due to alternative splicing, localizes throughout the mitotic spindle. Deletion of the C-terminal SxIP motifs (Shot Δ CT) results in primarily diffuse cytoplasmic localization. Treatment with Cyt-D does not reduce or enhance ShotA pole localization. (C) His-Arp-1 directly interacts with GST-Shot^{ABD} (comprising CH1–CH2 domains); the CH2 domain alone is insufficient for Arp-1 binding. ABD mutations L238A and L340P reduce and completely ablate Arp-1 binding, respectively. Shot C-terminus (aa 5071–5501) does not bind Arp-1. GST alone is also devoid of binding.

contain multiple modular domains that together confer the capability of physical association with all three cytoskeletal components (Figure 1A). Most spectraplakins contain tandem N-terminal calponin homology (CH) domains that bind F-actin (referred to here as the actin-binding domain, ABD) and C-terminal Growth Arrest Specific Protein 2 (GAS2) and SxIP domains that bind to the lattice and plus ends of MTs, respectively (Applewhite et al., 2010; Suozzi et al., 2012). The central spectrin repeats not only provide physical separation of actin- and MT-binding regions but are also considered to provide structural flexibility that may be important for accommodating the dynamic nature of the cross-linked components and contribute to Shortstop (Shot) autoinhibition (Applewhite et al., 2013).

Owing to their unique cytoskeletal cross-linking capacity, spectraplakins have been shown to participate in diverse cellular functions. The mammalian microtubule actin cross-linking factor 1 (MACF1), also called actin cross-linking factor 7 (ACF7), plays a crucial role in endodermal cell migration during wound healing, a process that requires both actin- and MT-binding functionalities (Kodama et al., 2003). Further studies in skin epidermis indicated an important role for ACF7 in maintaining proper dynamics of actin-based focal adhesions through physical coupling with MTs (Wu et al., 2008). Interestingly, ACF7 is capable of cross-linking and orienting noncentrosomal MTs to F-actin by regulating focal adhesion dynamics during migration of cultured human epithelial cells (Ning et al., 2016). A similar function has recently been described in specifying the anterior–posterior axis during *Drosophila* embryonic development (Nashchekin et al., 2016).

Studies on *Drosophila* Shortstop (Shot), the lone ACF7 orthologue in flies, have demonstrated a role in neuronal axon development.

Axons from both sensory and motor neurons in flies lacking Shot prematurely “stop short”; axon navigation requires an intact actin-binding functionality of Shot (Lee and Kolodziej, 2002; Bottenberg et al., 2009; Sanchez-Soriano et al., 2009). Furthermore, terminal arborization at neuromuscular junctions is defective, a result that is caused by improper MT organization (Prokop et al., 1998). Shot cytoskeletal cross-linking activity is required for proper photoreceptor development as well (Mui et al., 2011). Recent studies have identified an interaction with Patronin, an MT minus end-binding protein, which together with Shot promotes MT polarization required for apical–basal epithelial polarity as well as the oocyte anterior–posterior axis (Khanal et al., 2016; Nashchekin et al., 2016). Studies in *Drosophila* S2 cells have provided molecular insights into Shot’s role in dynamic cytoskeletal organization. GAS2 domain-mediated MT interactions are critical for stabilization against lateral movements. Cross-linking to actin filaments via the ABD maintains this MT-stabilizing effect (Applewhite et al., 2010). Interestingly, GAS2-mediated MT binding is autoinhibited before Shot activation at the MT plus end via the SxIP motif, and MT binding itself is dependent on an intact F-actin network (Applewhite et al., 2013).

These studies highlight a conserved role of spectraplakins in dynamic cytoskeletal cross-talk involved in cell migration and morphogenesis. However, these studies have all been conducted in nondividing cells, and thus the role of spectraplakins in cell division is unclear. Here we have investigated the mitotic functions of Shot in *Drosophila* S2 cells and the imaginal wing disk epithelium. We find that knockdown of Shot expression results in diverse mitotic defects, including unfocused spindle poles, defective spindle orientation, and compromised chromosome movements. Interestingly, the processes altered following Shot loss are all known to require activity of the Dynein/Dynactin complex. We find that an intact Shot^{ABD} is both necessary and sufficient for direct in vitro interaction with Actin-related Protein-1 (Arp-1), an integral component of the Dynactin complex structure required for Dynein activation (Kardon and Vale, 2009), and knockdown of Arp-1 universally phenocopies the loss of Shot in dividing cells. Chemical disruption of F-actin, however, only partially resembles the effects of Shot knockdown. Using *Drosophila* wing disk epithelia as an in vivo tissue model, we show that loss of Shot causes induction of apoptosis, the prevention of which generates an epithelial–mesenchymal transition (EMT)-like phenotype. Collectively our results demonstrate novel mitotic functions of Shot and suggest these are, at least partially, dependent on interaction with the Dynactin complex as opposed to its known F-actin cross-linking activity during interphase.

RESULTS

Shot localizes to mitotic spindle poles and MTs

We first examined the localization of Shot in mitotic S2 cells using fluorophore-tagged transgenes containing specific modular domains of the protein (Figure 1A). Full-length Shot fused to green

fluorescent protein (GFP:ShotA) predominantly localized to mitotic spindle poles (Figure 1B). GFP:ShotA signal was also noticeable in small puncta found localized along spindle MTs, including at or near the MT plus ends, suggesting Shot may have mitotic functions not only at spindle poles but also at MT tips similar to nondividing cells (Applewhite *et al.*, 2010). Interestingly, a splice isoform of Shot with a unique N-terminal sequence that also lacks the calponin homology 1 (CH1) domain, a critical part of the ABD (termed GFP:ShotC herein), localized throughout the mitotic spindle itself, likely mediated through intact MT-binding domains (MBDs) in the C-terminus (Figure 1B). Recombinant removal of the C-terminal, MT-binding SxIP motifs (mCherry:Shot Δ CT) resulted in a mostly diffuse cytoplasmic localization (Figure 1B). In contrast to exclusion of the complete ABD sequence in ShotC, treatment of cells with the mycotoxin cytochalasin-D (Cyt-D), which disrupts existing F-actin filaments and prevents further assembly, did not affect Shot localization at spindle poles or MTs either positively or negatively (Figure 1B). Altogether these results suggest that spindle poles represent a major site of Shot localization during mitosis, with a smaller fraction localizing to spindle MTs and that both ABDs and MBDs are required despite being independent of F-actin.

Shot directly binds the Dynactin component Arp-1

The persistence of Shot's spindle pole localization following Cyt-D treatment suggested its ABD may have additional interactions beyond F-actin filaments crucial to its mitotic function. We reasoned that Shot may operate at spindle poles through interaction with Arp-1, the key filamentous component of the Dynein-activating Dynactin complex (Kardon and Vale, 2009). Dynactin localizes to spindle poles in diverse cell types, where it contributes to bipolar spindle assembly (Gaglio *et al.*, 1997; Quintyne *et al.*, 1999). Additionally, cortically localized Dynactin contacts spindle MT asters to generate forces that determine spindle orientation (Siller *et al.*, 2005; Siller and Doe, 2008; Kotak *et al.*, 2012). β III-spectrin, a member of the spectrin family from which spectraplakins evolved (Suozi *et al.*, 2012), directly binds Arp-1 to activate Dynein/Dynactin-mediated vesicular transport. This interaction occurs through the tandem CH domains of β III-spectrin and is disrupted in spinocerebellar ataxia 5 (Holleran *et al.*, 2001; Ikeda *et al.*, 2006; Clarkson *et al.*, 2010). For examining this hypothesis directly, Shot tandem CH domains, the effective ABD, were expressed in *Escherichia coli* as a glutathione S-transferase (GST) fusion and immobilized on glutathione agarose resin. Arp-1 was expressed with an N-terminal His tag and purified via Ni²⁺-NTA and size-exclusion chromatographies. His-Arp1 directly bound GST-Shot^{ABD} in pull-down experiments (Figure 1C). Binding required both CH domains, as the CH2 alone was insufficient for Arp-1 interaction. Binding was significantly reduced in an L238A mutant, which is located within the canonical actin-binding region of CH1 (Levine *et al.*, 1992). An L340P mutation found within CH2, which is analogous to the allelic β III-spectrin mutation in cerebral ataxia (Clarkson *et al.*, 2010), completely abolished Shot^{ABD} binding to Arp-1 (Figure 1C). As an additional control, the C-terminus of Shot, which has no known actin-binding property, was used and showed no appreciable interaction with Arp-1. These results demonstrate the ability of the Shot^{ABD} to directly bind a key component of the Dynactin complex and establish a possible molecular mechanism for direct involvement in Dynein-dependent processes during mitosis.

Shot is required for proper mitotic spindle orientation

Our previous work identified a role for cortical actin in spindle orientation mediated through Frizzled/Dishevelled (Fz/Dsh), which induces Rho-dependent actin polymerization through noncanonical

signaling (Johnston *et al.*, 2013). Similar results were demonstrated in other reports investigating Wnt-dependent spindle positioning (Cabello *et al.*, 2010; Castanon *et al.*, 2012), as well as in those highlighting a generalized role of actin in this process (Kunda and Baum, 2009; Nestor-Bergmann *et al.*, 2014). We thus examined the role of Shot in spindle positioning as a potential novel component of this mitotic process. Polarized cortical crescents of Dsh were induced using the cell adhesion protein Echinoid as previously described, to which spindle orientation at metaphase was measured (Supplemental Figures S1 and 2A) (Johnston *et al.*, 2009). Whereas control cells orient their spindle preferentially toward the center of the Ed:Dsh crescent, treatment with double-stranded RNA (RNA interference [RNAi]) targeted against the coding region of Shot randomized spindle orientation (Supplemental Figure S1). We next examined whether Shot^{RNAi} could also perturb spindle orientation relative to Pins, a spindle-positioning cue not known to directly influence cortical actin, using the same reconstitution system. Indeed, Shot^{RNAi} disrupted Pins-mediated spindle positioning in a manner similar to that seen with Dsh (Figure 2, A and B), suggesting Shot plays a more generalized role in this process. Because Pins likely represents a more universal spindle orientation cue (Lu and Johnston, 2013), and has a more robust activity in the induced polarity assay, we chose to focus our efforts on it for the remainder of our studies.

We next examined the structure–function relationship of Shot-dependent spindle orientation using a set of recombinant rescue constructs. Cells were treated with RNAi directed against the 3' untranslated region (UTR) of Shot to reduce endogenous expression and transfected with RNAi-resistant Shot transgenes as potential rescue constructs. As shown in Figure 2C, full-length Shot (ShotA) was able to rescue Pins-mediated spindle orientation. In contrast, a Shot isoform lacking the N-terminal actin-binding domain (ShotC) was incapable of rescue. Removing the C-terminal MT-associating "SxIP" motifs (Shot Δ CT) also prevented rescue activity (Figure 2C). These results demonstrate that Shot, and more specifically both its actin- and MT-binding regions, is necessary during cell division for proper positioning of the mitotic spindle.

Several studies have demonstrated a role for the actin cortex in mitotic spindle assembly and orientation, a role seemingly conserved from yeast to human cells (Kunda and Baum, 2009). To determine the role of F-actin in our Ed:Pins-based S2 cell system, we treated cells with Cyt-D; acute treatment resulted in spindle orientation randomization, indicating that cortical actin is necessary for Pins function in this system (Figure 2B). Treatment with Arp-1^{RNAi} also uncoupled spindle orientation from Ed:Pins, as did treatment with RNAi directed against the Dynein heavy-chain Dhc64C (Figure 2B). We confirmed that both Shot and Dhc64C RNAi constructs were highly effective at protein knockdown using Western blot analysis (Supplemental Figure S2), although no suitable antibody was identified for examining Arp-1 levels. We also performed double Shot^{RNAi}/Arp-1^{RNAi} and Shot^{RNAi}/Dhc64C^{RNAi} treatments and found these to be statistically indistinguishable from any single RNAi condition (Figure 2D). Whether Shot functions through F-actin filaments or Arp-1 to regulate spindle positioning cannot be completely deduced, although localization of ShotA, the only isoform that supports spindle orientation, is F-actin-independent in mitotic cells (Figure 1B), and loss of Shot is not synthetic with Arp-1 or Dhc64C loss, suggesting Arp-1 may be more relevant to its function.

Shot is required for bipolar spindle assembly

To determine whether Shot affects other aspects of spindle function beyond spatial orientation, we examined spindle assembly following Shot knockdown. Shot^{RNAi} treatment resulted in a significant increase

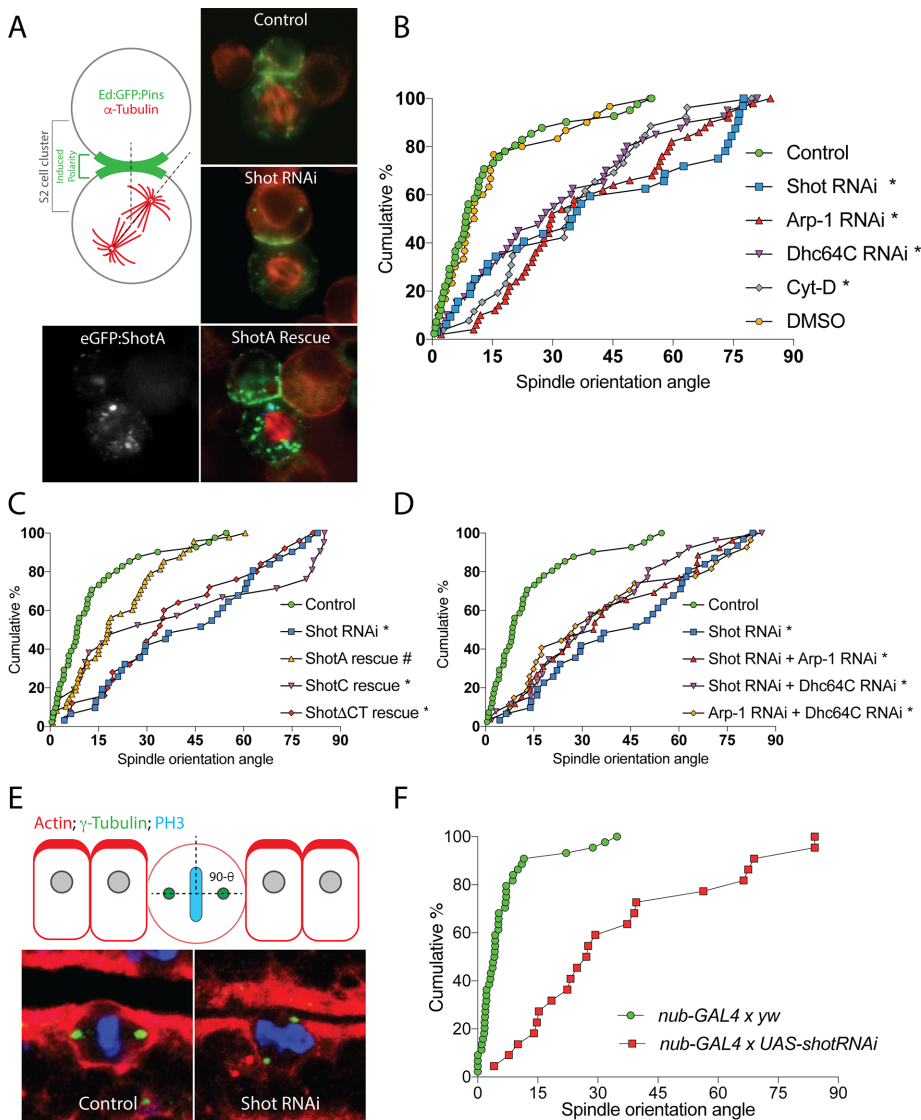


FIGURE 2: Shot is required for mitotic spindle orientation. (A) S2 cells transfected with Ed:GFP:Pins (or Ed:FLAG:Pins pseudocolored green for ShotA rescue) were induced to form small (two to three cells) clusters that cortically polarize Pins at sites of cell contact. The orientation of the induced mitotic spindle (marked by α -tubulin in red) was measured relative to the center of the induced Pins crescent. Representative images are shown for control, Shot^{RNAi}-mediated loss of spindle orientation, and ShotA rescue of the Shot^{RNAi} phenotype. (B) Graph of cumulative percentage of measurements vs. spindle angle demonstrating the loss of activity following RNAi directed against Shot, Arp-1, or Dhc64C. Treatment of cells with Cyt-D also prevents proper spindle orientation, whereas DMSO was without effect. Symbols represent individual measurements taken from at least three independent experiments. *, $p < 0.05$ compared with control; analysis of variance (ANOVA), Tukey's post hoc test. (C) Expression of RNAi-resistant Shot rescue transgenes demonstrates the necessity of both actin- and MT-binding functions in spindle orientation. ShotA, but not ShotC or Shot Δ CT, is capable of rescuing Ed:Pins-mediated spindle orientation in the absence of endogenous Shot expression (generated with RNAi against the Shot 3'-UTR). Symbols represent individual measurements taken from at least three independent experiments. *, $p < 0.05$ compared with control; #, $p < 0.05$ compared with Shot^{RNAi}; ANOVA, Tukey's post hoc test. (D) Combined treatment with Shot, Arp-1, and Dhc64C RNAi does not differ from any single RNAi treatment alone. Symbols represent individual measurements taken from at least three independent experiments. *, $p < 0.05$ compared with control; ANOVA, Tukey's post hoc test. (E) Epithelial cells of the *Drosophila* imaginal wing disk normally orient spindles parallel to actin-dense folds. Shown are representative images for control and Shot^{RNAi}-expressing cells. (F) Cumulative percentage graph depicting the magnitude of spindle orientation loss following Shot^{RNAi} expression. Shot^{RNAi} expression caused a significant reduction in spindle orientation accuracy. $p < 0.05$, Student's *t* test.

in cells with abnormal spindle morphology. Specifically, one or both spindle poles were often unfocused, with K-fibers splayed at their ends despite the presence of an intact, γ -tubulin-positive centrosome, with Shot^{RNAi} inducing a 2.05-fold increase in K-fiber spread distance (Figure 3B). The number of spindle poles was not significantly altered by Shot loss, and the predominant phenotype could be described as bipolar, unfocused spindles (Figure 3A). We next performed rescue experiments to determine the structure-activity relationship of Shot-dependent pole focusing. As with spindle orientation, full-length Shot (ShotA) expression conferred a significant rescue effect, whereas constructs lacking the ABD (ShotC) or MBD (Shot Δ CT) were devoid of rescue activity for spindle pole focusing (Figure 3B). Cells treated with Cyt-D had a smaller but significant increase in unfocused spindle poles (1.67-fold increase). Treatment with Arp-1^{RNAi} and Dhc64C^{RNAi} resulted in 1.99- and 1.74-fold increases in pole distance, respectively (Figure 3B). As with spindle orientation, double RNAi treatments of Shot together with either Arp-1 or Dhc64C (or Arp-1 and Dhc64C together) did not result in further worsening of pole focusing (Figure 3B), suggesting these factors may function together within the same pathway. Thus Shot is critical for proper spindle pole focusing, potentially through interactions with F-actin, Dynein/Dynactin, or both. Several studies have demonstrated that normal spindle pole focusing occurs through overlapping activities of minus-end microtubule motors, including the Dynein/Dynactin complex (Gaglio *et al.*, 1996; Walczak *et al.*, 1998; Merdes *et al.*, 2000; Maiato *et al.*, 2004; Goshima *et al.*, 2005; Morales-Mulia and Scholey, 2005). Although cortical actin has been shown to contribute to centrosome dynamics and spindle assembly in some systems (Moulding *et al.*, 2007; Carreno *et al.*, 2008; Kunda *et al.*, 2008; Sandquist *et al.*, 2011), additional evidence suggests its main role is cell rounding, rather than a direct role per se, and is therefore dispensable in isolated, nonconfined cells (Lancaster *et al.*, 2013). Furthermore, normal bipolar spindles can form in cell extracts that are likely devoid of F-actin filaments (Heald *et al.*, 1996).

Shot is required for timely chromosome congression necessary for anaphase onset

To identify additional mitotic functions of Shot, particularly those known to depend on Dynactin/Dynein activity, we next

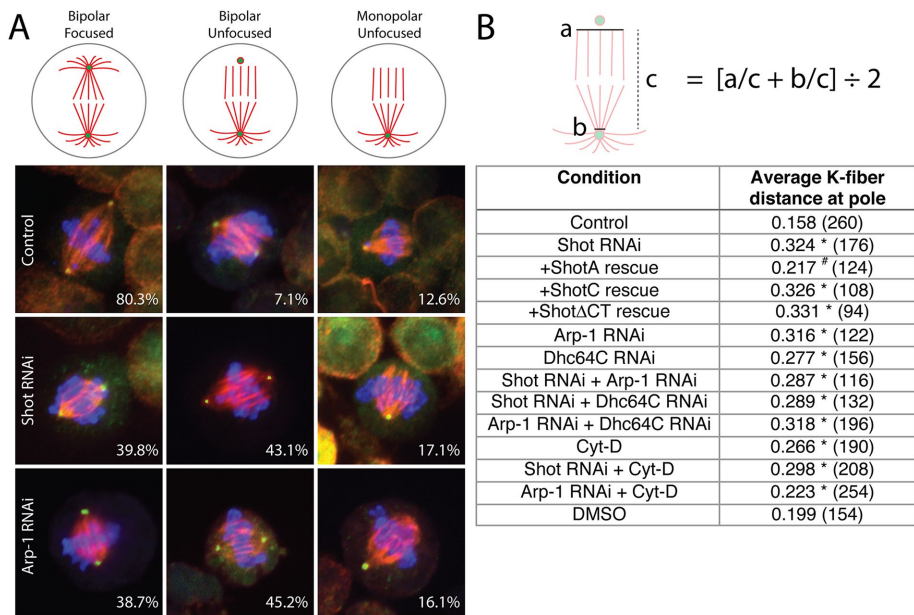
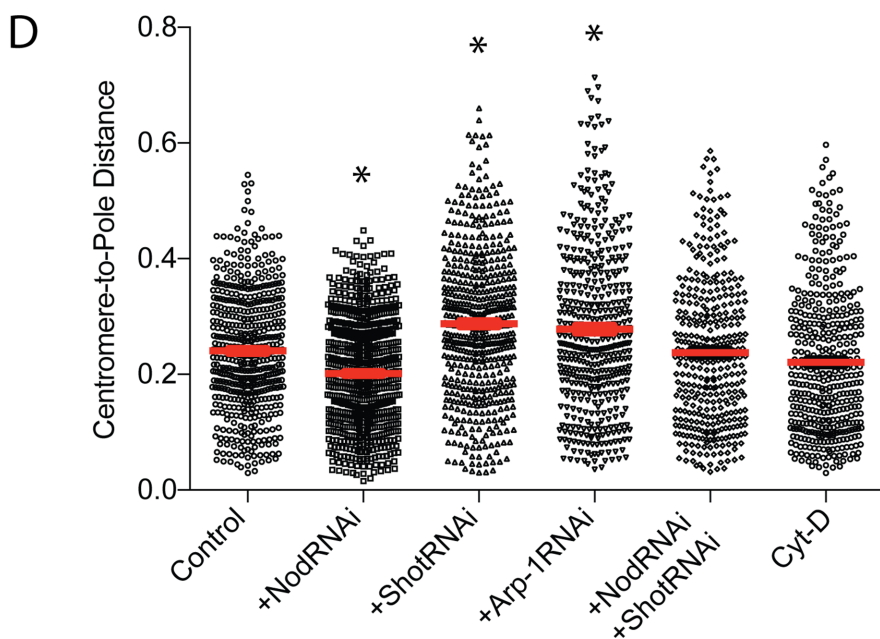
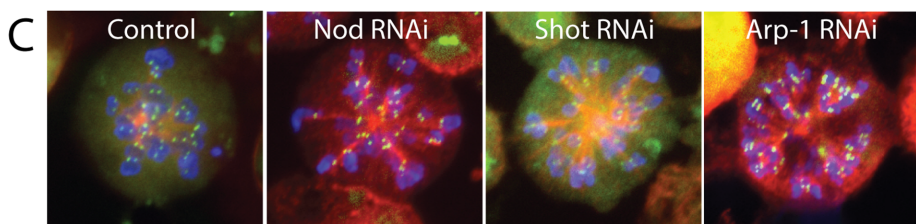
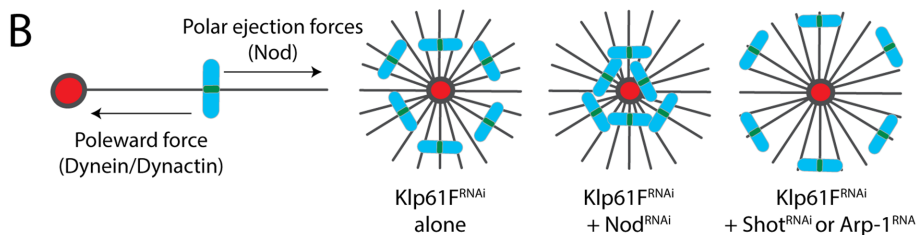
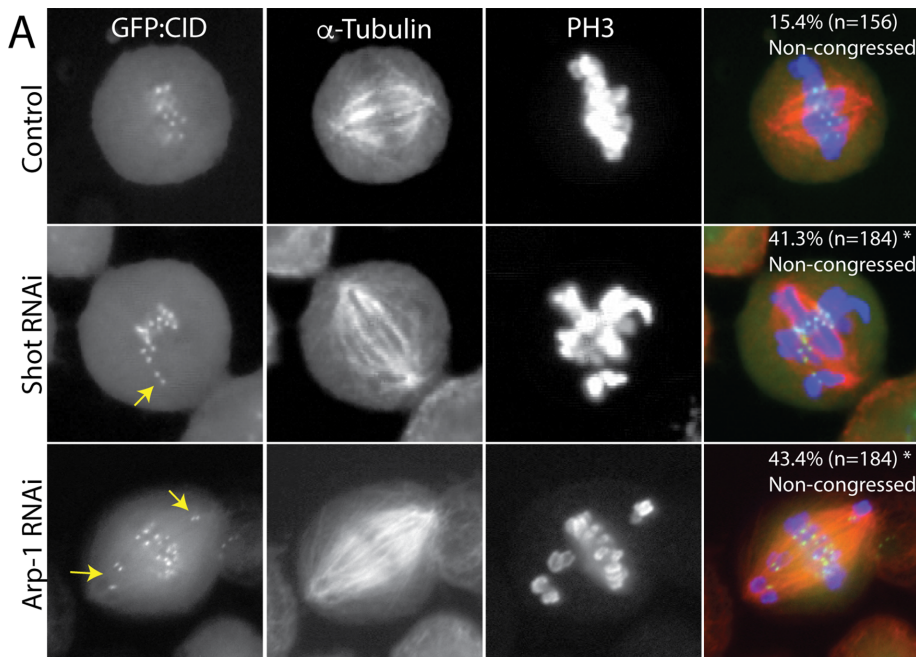


FIGURE 3: Shot is required for focusing of mitotic spindle poles. (A) Three significant phenotypes were observed for spindle morphology: “Bipolar Focused” as normal, “Bipolar Unfocused” in which one or both poles are unfocused although two γ -tubulin positive centrosomes are still present, and “Monopolar Unfocused” in which one unfocused pole is devoid of a γ -tubulin-positive centrosome. Representative images are shown for control, Shot^{RNAi}-treated, and Arp-1^{RNAi}-treated S2 cells with α -tubulin marked red, γ -tubulin marked green, and PH3 marked blue. Shot^{RNAi} and Arp-1^{RNAi} each lead to a selective increase in “Bipolar Unfocused” spindles at the expense of “Bipolar Focused.” (B) Table summarizing all conditions tested. Data represent the average width of both spindle poles divided by spindle length. Numbers in parentheses are the total number of cells measured for each condition. Only ShotA was capable of rescuing spindle pole focusing. Shot^{RNAi} was indistinguishable from both Arp-1^{RNAi} and Dhc64C^{RNAi}. Double RNAi treatments were not significantly worse than single RNAi treatments, nor was combination treatment with Cyt-D. Statistical analyses were performed with ANOVA followed by Tukey’s post hoc test (*, $p < 0.05$ compared with control; #, $p < 0.05$ compared with Shot^{RNAi}).

examined chromosome congression (Sharp *et al.*, 2000; Yang *et al.*, 2007). Following nuclear envelope breakdown, microtubule plus ends search and capture chromosome kinetochores, which must then be correctly congressed to the metaphase plate and properly aligned to ensure timely cell cycle progression and accurate segregation at anaphase. Complete congression of polar chromosomes to the spindle equator requires a coordinated effort of Aurora kinases, the CENP-E kinesin motor, and Dynein (Kim *et al.*, 2010). Dynein is necessary to oppose polar ejection forces (PEFs), generated by plus end-directed kinesin motors, allowing for a net minus-end movement of chromosomes along astral microtubules to spindle poles (Barisic *et al.*, 2014). Whereas control S2 cells typically did not show chromosomal congression defects (15.4%, $n = 156$), Shot^{RNAi} treatment resulted in cells frequently having noncongressed, pole-localized chromosomes at metaphase (43.5%, $n = 184$), which were visualized using the histone-like centromere marker, Centromere Identifier (*Drosophila* orthologue of CENP-A), fused to GFP (GFP:CID) (Figure 4A). RNAi directed against Arp-1 resulted in a similar congression defect (41.3%, $n = 184$), as did treatment with Dhc64C^{RNAi} (54.3%, $n = 280$). In contrast, Cyt-D treatment did not significantly increase the incidence of defective congression relative to control (18.5%, $n = 173$), suggesting that this Shot phenotype is strictly independent of F-actin interactions. Furthermore, Shot^{RNAi}/Arp-1^{RNAi} and Shot^{RNAi}/Dhc64C^{RNAi} double knockdowns did not significantly differ from any single RNAi treatment condition (49.6%, $n = 354$, and 51.5%, $n = 518$, respectively).

To quantify this effect more precisely, we induced monopolar spindles using RNAi against Klp61F, the *Drosophila* orthologue of the Eg5 kinesin required for separation of duplicated centrosomes and spindle bipolarity (Sawin *et al.*, 1992), and measured the distance from GFP:CID-positive centromeres to the center of this single pole (Figure 4B). Shot^{RNAi} and Arp-1^{RNAi} caused similar and statistically significant increases in this centromere–pole distance relative to control (Figure 4, C and D). Increased distance from the pole is consistent with overwhelming PEFs in the absence of minus-end movements through Dynein (Barisic *et al.*, 2014). To test this, we treated cells with RNAi against the PEF-generating chromokinesin, Nod. As expected, treatment with Nod^{RNAi} alone reduced the centromere–pole distance, consistent with unopposed Dynein function. Under double-knockdown conditions, Shot^{RNAi} suppressed the effects of Nod^{RNAi}, yielding an intermediate distance similar to control cells (Figure 4D). Finally, treatment of cells with Cyt-D did not significantly affect chromosome distance relative to control, again indicating that F-actin does not play an essential role in this process under these experimental conditions. These findings collectively suggest a model in which Shot aids in Dynein-mediated chromosome forces that permit poleward transport, presumably through an interaction with Arp-1.

Proper chromosome congression and alignment are necessary for timely anaphase onset and mitotic exit. Once chromosomes congress and become bi-oriented at the metaphase plate, Dynein-mediated forces are used to remove components of the spindle assembly checkpoint (SAC) from kinetochores, triggering anaphase onset, and to subsequently help separate sister chromatids to their respective spindle poles during anaphase (Howell *et al.*, 2001; Bader and Vaughan, 2010). To determine whether Shot has a role in cell cycle timing, we measured the time from nuclear envelope breakdown (NEB) to anaphase onset using live-cell imaging of S2 cells expressing GFP:CID and α -tubulin:mCherry. Anaphase onset in control cells occurred 47.8 ± 18.9 ($n = 8$) min following NEB. Knockdown of Shot, Arp-1, or Dhc64C each resulted in significant delay of anaphase onset, with the majority of cells experiencing metaphase arrest (five out of seven, five out of nine, and eight out of nine, respectively; Figure 5B). Overall Shot^{RNAi} increased NEB–anaphase timing to 143.8 ± 63.05 ($n = 7$) min, whereas Arp-1^{RNAi} and Dhc64C^{RNAi} had similar average timings of 126.4 ± 63.05 ($n = 9$) and 176.4 ± 10.7 ($n = 9$) min to anaphase onset (Figure 5). Cells arrested in metaphase failed to enter anaphase even after 180 min, the time point at which we stopped imaging due to photobleaching and concerns of phototoxicity, and suggesting that these numbers may underrepresent the magnitude of the anaphase delay in RNAi-treated cells. To corroborate these live-cell results, we also measured the mitotic index in respective fixed cell populations: control cells 2.1% ($n = 3488$), Shot^{RNAi} cells 9.1% ($n = 2539$), Arp-1^{RNAi} cells 8.6% ($n = 2361$), and Dhc64C^{RNAi} cells 8.8% ($n = 3014$). These results are consistent with previous



reports (Morales-Mulia and Scholey, 2005) and further substantiate the effects of Shot loss on mitotic exit. To differentiate between the potential roles of F-actin and Arp-1 in Shot-dependent cell cycle progression, we examined effects of Cyt-D on anaphase timing. In contrast to Arp-1 loss, treatment with Cyt-D did not significantly affect NEB-anaphase timing (29.4 ± 8.6 min, $n = 12$; Figure 5B). We also examined RNAi against β III-spectrin, which also binds Arp-1, but for the purpose of vesicular traffic in nondividing cells. This treatment did not significantly increase cell cycle timing, indicating specificity in Arp-1-binding interactions.

To ascertain whether activation of the SAC was responsible for this delay, we used RNAi against Rod, a member of the RZZ

FIGURE 4: Shot is required for poleward congression of mitotic chromosomes. (A) S2 cells stably expressing GFP:CID were treated with control, Shot^{RNAi}, or Arp-1^{RNAi} and visualized using antibodies against α -tubulin (red) and PH3 (blue). Shot^{RNAi} and Arp-1^{RNAi} each significantly increase the percent of cells with noncongressed chromosomes (*, $p < 0.05$; ANOVA with Tukey's post hoc test). Percent of cells with noncongressed chromosomes for additional conditions not shown: Dhc64C^{RNAi} = 54.3% ($n = 280$), $p < 0.05$; Shot^{RNAi} + Arp-1^{RNAi} = 49.7% ($n = 312$), $p < 0.05$; Shot^{RNAi} + Dhc64C^{RNAi} = 51.5% ($n = 518$), $p < 0.05$; Arp-1^{RNAi} + Dhc64C^{RNAi} = 50.8% ($n = 354$), $p < 0.05$; and Cyt-D = 18.5% ($n = 173$), not significant. Double RNAi treatments did not significantly differ from single RNAi treatments. (B) Schematic depicting Klp61^{RNAi}-mediated monopolar spindle assay. Chromosomes move along monopolar asters by means of two opposing forces: a plus-end PEF generated by the chromokinesin Nod, and a minus-end "poleward force" generated by Dynein/Dynactin. Loss of PEF or poleward forces is predicted to result in a decrease or increase in pole-to-chromosome distance, respectively. (C) Representative images for selective experimental conditions illustrate monopolar microtubules marked with α -tubulin (red), mitotic chromosomes marked with PH3 (blue), and centromeres marked with GFP:CID (green). (D) Plots for all data collected across each experimental condition. Whereas Nod^{RNAi} decreased centromere-to-pole distance, both Shot^{RNAi} and Arp-1^{RNAi} resulted in an increase in this metric. Cotreatment with Nod^{RNAi} and Shot^{RNAi} resulted in an intermediate distance. Cyt-D was without significant effect. *, $p < 0.05$; ANOVA with Tukey's post hoc test.

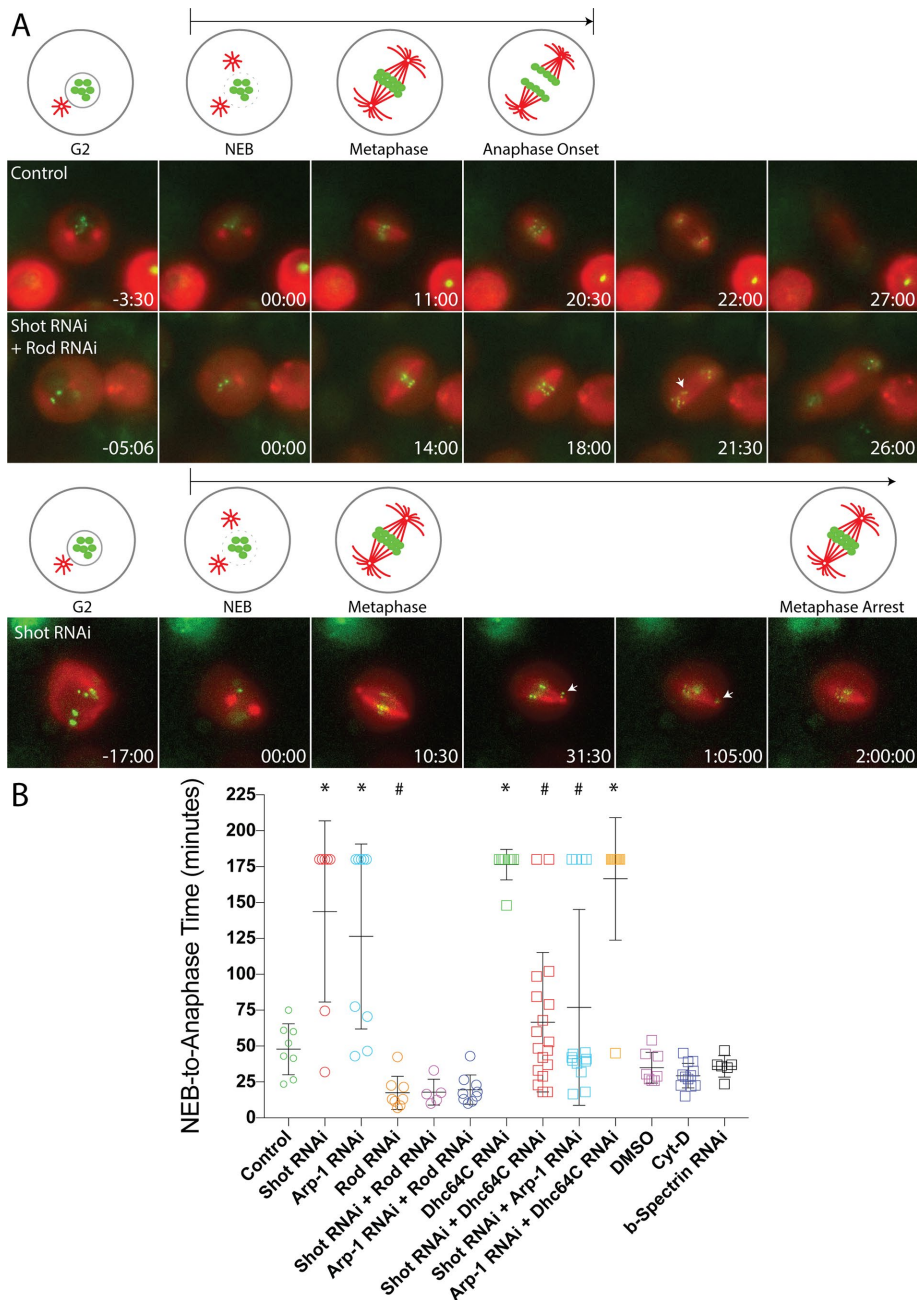
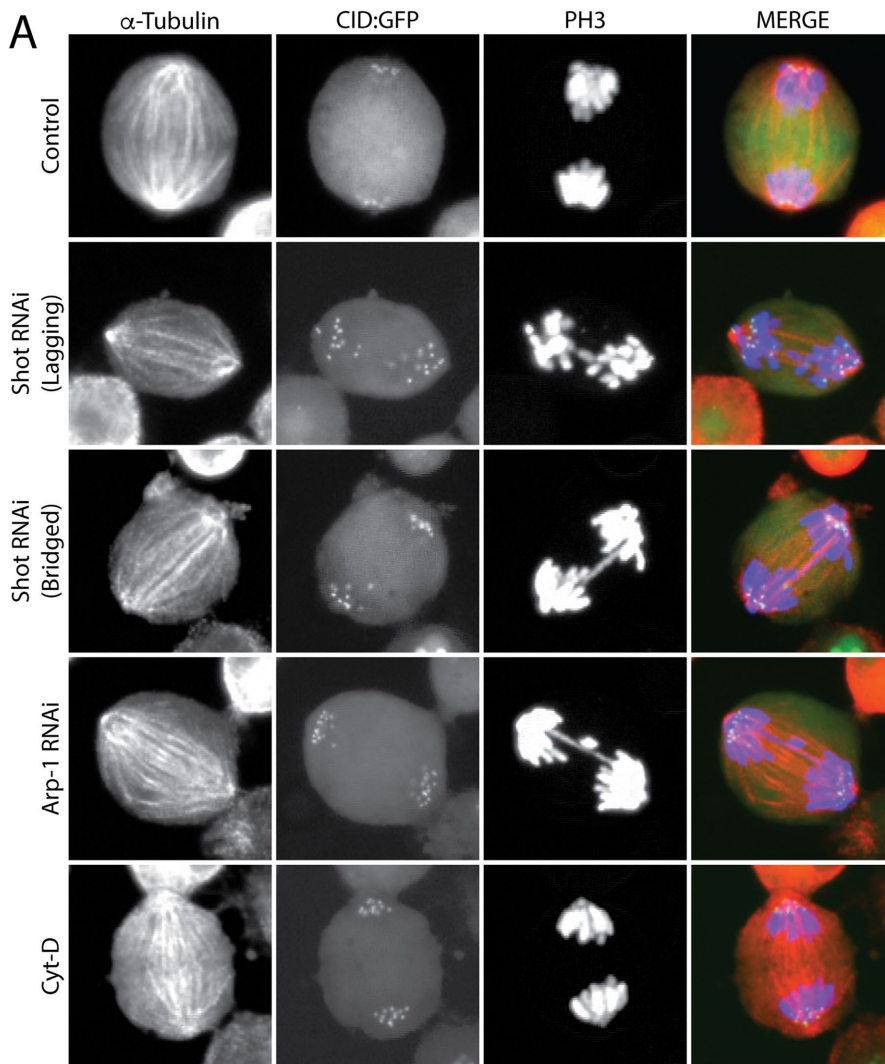


FIGURE 5: Shot loss activates the SAC to delay mitotic exit. (A) Live-cell imaging was conducted on S2 cells stably expressing inducible GFP::CID and mCherry:: α -tubulin. Images are shown from representative movies of control, Shot^{RNAi}-treated, and Shot^{RNAi}/Rod^{RNAi}-cotreated cells at indicated time points relative to NEB. Whereas control and double-mutant cells progress to anaphase within ~20 min, Shot^{RNAi}-treated cells frequently undergo metaphase arrest. The arrow in the Shot^{RNAi}/Rod^{RNAi} anaphase image indicates a lagging chromosome. The arrows in metaphase images of Shot^{RNAi} highlight a noncongressed chromosome that remains at the spindle pole. (B) Plot of NEB-to-anaphase timing for all movies taken from indicated experimental conditions. Shot^{RNAi}, Arp-1^{RNAi}, and Dhc64C^{RNAi} each induces a significant delay that results from cells frequently arresting in metaphase. Loss of the SAC component Rod suppressed both the Shot^{RNAi}- and Arp-1^{RNAi}-mediated metaphase arrest phenotype. Combined treatments of Shot^{RNAi}/Arp-1^{RNAi} or Shot^{RNAi}/Dhc64C^{RNAi} caused a suppression of metaphase arrest seen in single RNAi conditions, whereas Arp-1^{RNAi}/Dhc64C^{RNAi} dual treatment did not differ from either treatment alone. Cyt-D did not affect cell cycle timing, nor did RNAi against the spectrin protein β III-spectrin. Data points are measured from individual cell divisions representing at least three independent experiments. *, $p < 0.05$ compared with control; #, $p < 0.05$ compared with Shot^{RNAi} alone; ANOVA with Tukey's post hoc test.

complex and a key component of the SAC (Basto *et al.*, 2000). Indeed, Rod^{RNAi} suppressed the effects of both Shot^{RNAi} and Arp-1^{RNAi} by shortening anaphase onset timing to a level similar to Rod^{RNAi} alone, which was slightly hastened compared with control cells (Figure 5). These results suggest that Shot functions together with Arp-1 to promote Dynein-mediated cell cycle timing by aiding in the proper silencing of the SAC necessary for mitotic checkpoint inactivation and anaphase transition. Surprisingly, when cells were treated with a combination of Shot^{RNAi} and Arp-1^{RNAi} (or Shot^{RNAi} and Dhc64C^{RNAi}) the anaphase onset delay seen in each single RNAi treatment was suppressed, and only a minority of cells in these conditions experienced metaphase arrest (Figure 5B). Concordantly, the mitotic index in the Shot/Arp-1 double knockdown was significantly reduced (4.1%, $n = 3600$), while the Shot/Dhc double knockdown caused an even more complete reversal (2.8%, $n = 3383$). Treatment with an Arp-1^{RNAi}/Dhc64C^{RNAi} combination did not, however, differ from single RNAi treatments in either metric, indicating the loss of cell cycle arrest in Shot double knockdowns is not due to nonspecific effects such as RNA toxicity.

Shot is required for proper chromosome segregation during anaphase but not for cytokinesis

We next examined whether loss of Shot, in addition to delaying anaphase onset, might also impact chromosome segregation once anaphase commences. We again used S2 cells stably expressing GFP::CID to quantify the incidence of chromosome segregation errors. Control cells showed a moderate incidence of lagging or bridged chromosomes (23.7%, $n = 169$). Shot^{RNAi} treatment significantly increased segregation defects (42.4%, $n = 172$; Figure 6). Arp-1^{RNAi} and Dhc64C^{RNAi} treatments resulted in similar effects (63.9%, $n = 161$, and 49.8%, $n = 241$, respectively), although the effects of Arp-1^{RNAi} were more prominent (Figure 6). Cyt-D, however, did not lead to significant chromosome segregation errors (23.1%, $n = 186$), nor did it alter the effects of Shot^{RNAi} and Arp-1^{RNAi} when treated in combination (Figure 6B). These results collectively suggest that Shot participates in chromosome segregation independent of F-actin and may rather function in Dynein/Dynactin-mediated poleward forces (Sharp *et al.*, 2000). Double RNAi treatment against Shot/Arp-1 or Shot/Dhc64C each resulted in elevated levels of segregation defects relative to single knockdowns (75.1%, $n = 218$, and



Condition	% cells with lagging or bridged chromosomes (n)	ANOVA: *, $p < 0.05$ to Control #, $p < 0.05$ to ShotRNAi
Control	23.7 (169)	-
Shot RNAi	42.4 (172)	*
Arp-1 RNAi	63.9 (161)	*,#
Dhc64C RNAi	49.8 (241)	*
Shot RNAi + Arp-1 RNAi	75.1 (354)	*,#
Shot RNAi + Dhc64C RNAi	81.6 (223)	*,#
Arp-1 RNAi + Dhc64C RNAi	58.3 (240)	*
Shot RNAi + Cyt-D	43.1 (174)	*
Arp-1 RNAi + Cyt-D	54.3 (162)	*
Cyt-D	23.1	#

FIGURE 6: Shot loss induces chromosome segregation defects. (A) GFP:CID-expressing S2 cells were fixed and marked with α -tubulin (red) and PH3 (blue) antibodies. Representative images are shown for indicated conditions. Control and Cyt-D-treated cells undergo mostly normal anaphase chromosome segregation, whereas Shot^{RNAi} and Arp-1^{RNAi} both induce lagging and bridged chromosomes. (B) Table shows quantification of defective segregation phenotype for all conditions tested. Treatment with Arp-1^{RNAi} or Dhc64C^{RNAi} had resulted in phenotypes similar to Shot^{RNAi}, although Arp-1^{RNAi} effects are significantly stronger. Cyt-D treatment, however, did not affect chromosome segregation, nor did it potentiate either Shot^{RNAi} or Arp-1^{RNAi} effects. Although combination RNAi treatment against Arp-1 and Dhc64C was not worse than either alone, concomitant loss of Shot and Arp-1 or Shot and Dhc64C was significantly worse than either condition alone. *, $p < 0.05$ compared with control; #, $p < 0.05$ compared with Shot^{RNAi} alone; ANOVA with Tukey's post hoc test.

81.6%, $n = 223$, respectively; Figure 6B). We believe that these results are a direct result of the loss of metaphase arrest described earlier for these conditions. Loss of Shot, Arp-1, or Dhc alone likely triggers anaphase delay due to defective chromosome congression and alignment. Slippage from the SAC under these double RNAi treatments could thus explain the high rates of segregation errors.

Finally, to assess the role of Shot and Arp-1 in cytokinesis, we quantified the percentage of binucleated S2 cells with the understanding that failed cytokinesis results in retention of both daughter nuclei in the original mother cell. Control cells were 1.18% binucleated ($n = 1348$). RNAi against Shot or Arp-1 each resulted in a small but insignificant increase in binucleated cells to 2.28% ($n = 1097$) and 2.98% ($n = 1508$), respectively, suggesting that neither of these components is critical for completing cytokinesis. In contrast, treatment with Cyt-D to ablate cortical F-actin, which is a well-established component of the cleavage furrow and contractile ring (Glotzer, 2005), resulted in a significant increase to 43.7% ($n = 958$) binucleated cells. Thus Shot plays an important role in chromosome dynamics and mitotic exit but does not appear to regulate the actomyosin ring function during cleavage furrow ingression and cytokinesis.

Shot is required for proper epithelial cell divisions in vivo

Having elucidated several novel mitotic functions of Shot in vitro, we sought to investigate how Shot participates in proper development of an animal tissue in vivo. To do so, we used imaginal wing disks from third instar *Drosophila* larvae, the predecessors to the adult wing structure that represent an excellent epithelial cell model and have been used extensively in the study of tissue growth and homeostasis (Hariharan, 2015). We first examined whether Shot participates in spindle orientation in this tissue. Wing disks display a characteristic pattern of actin-rich folds, and we have shown that adjacent cells normally orient their spindles parallel to these folds (Figure 2E) (Dewey et al., 2015). We expressed short hairpin RNA against Shot using *Nubbin-GAL4* (*nub>GAL4*) that drives expression ubiquitously in the wing disk pouch. Shot^{RNAi} randomized spindle orientation (Figure 2, E and F), demonstrating its role in oriented cell division is relevant in animal tissue. The effects of Shot^{RNAi} were similar in magnitude to RNAi against Mud, a previously identified spindle-orienting component in these cells (Nakajima et al., 2013; Dewey et al., 2015). Recent studies have

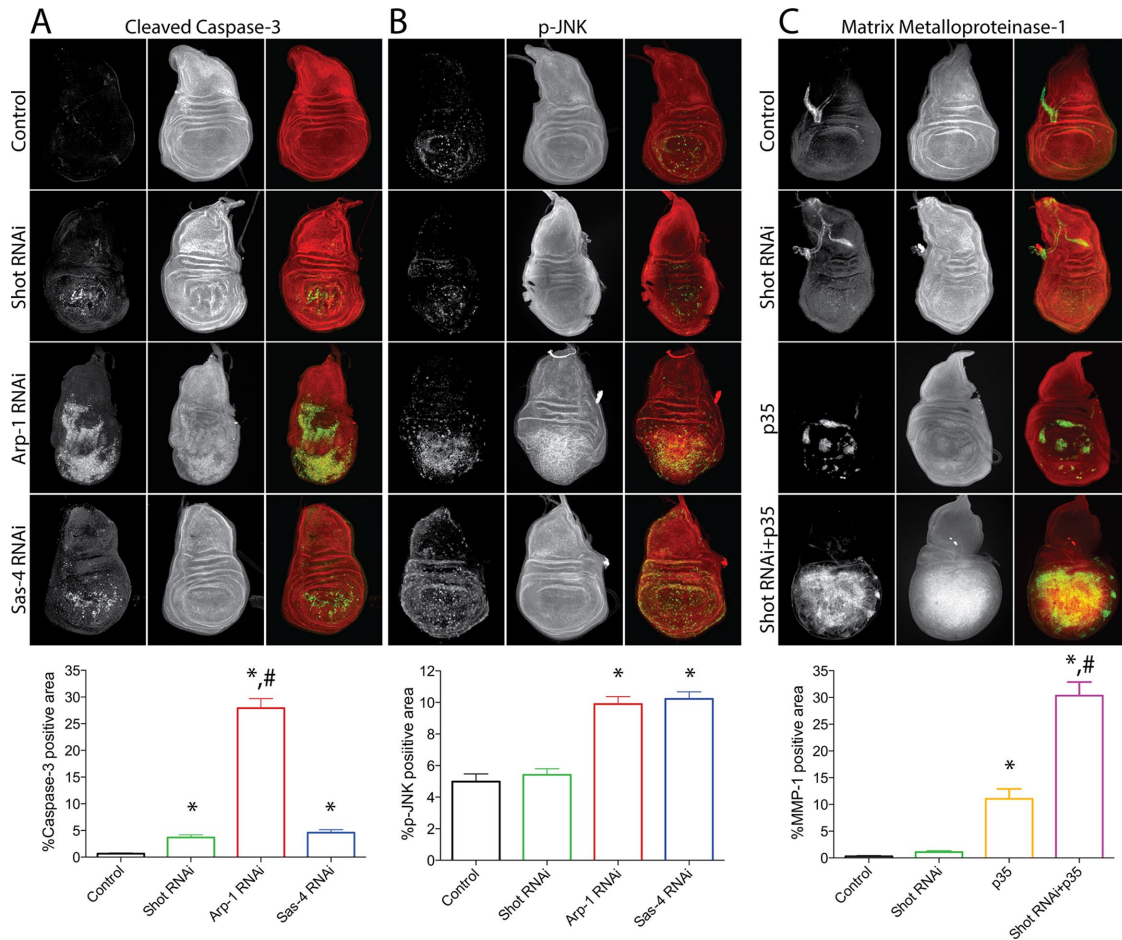


FIGURE 7: Shot loss activates apoptosis in *Drosophila* epithelia and leads to disruption of tissue morphology.

(A) Imaginal wing disks were dissected from late-stage L3 larvae, fixed, and stained for Cleaved Caspase-3 (green) and Alexa Fluor 568–phalloidin (red) to stain F-actin. Shot^{RNAi} causes an increase in apoptotic cells similar in magnitude to Sas-4^{RNAi}. Arp-1^{RNAi} induces a strikingly more significant apoptotic response. Shot^{RNAi} and, more so, Arp-1^{RNAi} often lead to noticeable alterations in the morphology of F-actin folds. *, $p < 0.05$ compared to Control and #, $p < 0.05$ compared to Shot^{RNAi}, ANOVA. (B) Imaginal wing disks were dissected from late-stage L3 larvae, fixed, and stained for phosphorylated-JNK (green) and Alexa Fluor 568–phalloidin (red). Whereas Shot^{RNAi} does not increase p-JNK levels, Arp-1^{RNAi} and Sas-4^{RNAi} cause a similar degree of increase. *, $p < 0.05$ compared to Control, ANOVA. (C) Imaginal wing disks were dissected from late-stage L3 larvae, fixed, and stained for Matrix metalloproteinase (green) and Alexa Fluor 568–phalloidin (red). Shot^{RNAi} alone does not significantly affect MMP-1, whereas expression of the antiapoptotic protein p35 leads to a moderate increase. Coexpression of Shot^{RNAi} and p35 leads to a dramatic and synergistic increase in MMP-1 expression as well as significant deformation in F-actin morphology. *, $p < 0.05$ compared to Control and #, $p < 0.05$ compared to p35, ANOVA.

shown that centrosome loss (following RNAi against SAS-4) also disrupts spindle orientation in wing disks (Poulton *et al.*, 2014), whereas supernumerary centrosomes induce only a mild disruption (Sabino *et al.*, 2015). Despite abnormal spindle positioning, centrosome numbers in wing disks expressing Shot^{RNAi} were not altered, with all cells containing two γ -tubulin–positive structures, consistent with results from S2 cells.

We next sought to determine the consequences of Shot loss on tissue development. We first examined apoptosis using cleaved caspase-3 as a molecular marker. Expression of Shot^{RNAi} resulted in an increased apoptosis similar to other genes that have recently shown to induce apoptosis in wing disks, including the centrosomal protein Sas-4 (Figure 7A) (Poulton *et al.*, 2014). In contrast to Sas-4, however, loss of Shot did not increase the expression of phosphorylated (activated) JNK, suggesting a JNK-independent mode of cell death (Figure 7B). Interestingly, Arp-1^{RNAi} also induced apoptosis; however,

its effects were significantly more dramatic than any of the other conditions examined (Figure 7A). Shot^{RNAi}, and to an even greater extent Arp-1^{RNAi}, also caused morphological abnormalities in the F-actin–dense folds of the wing pouch, indicating that their loss is detrimental to the overall tissue architecture (Figure 7A). To understand the importance of cell death in these contexts, we expressed the apoptosis inhibitor, p35. We also generated double transgenic lines that express p35 simultaneously with Shot^{RNAi}. We quantified the area of tissue expressing Matrix metalloproteinase 1 (MMP-1), a key marker of EMT, under these conditions. Expression of p35, but not Shot^{RNAi} alone, resulted in induction of MMP-1 expression. Coexpression of p35 with Shot^{RNAi} resulted in a marked and synergistic expression of MMP-1 (Figure 7C). These results indicate that, although apoptosis following Shot loss can lead to mild defects in epithelial tissue architecture, it is likely a response to prevent more substantive alterations should Shot-defective cells be allowed to persist.

DISCUSSION

Spectraplakins are large, modular scaffolds that facilitate dynamic cross-linking interactions between components of the cellular cytoskeleton. These proteins have well-established roles in facilitating cell migration, organizing multicellular tissue structures, and maintaining MT organization (Applewhite *et al.*, 2010; Suozzi *et al.*, 2012). Although remarkably diverse, these functions all contribute to activities that primarily operate in nondividing cells. We have shown here that Shot, the lone *Drosophila* spectraplakins gene, also plays an important role in mitotic cells. Specifically, loss of Shot results in a multifaceted phenotype characterized by unfocused mitotic spindle poles, misaligned spindles, and defective chromosome dynamics. Shot loss frequently leads to metaphase arrest, which is likely due to activation of the SAC. These diverse mitotic processes all share a common trait in their dependence on the force-generating MT motor protein Dynein (Raaijmakers *et al.*, 2013; Prosser and Pelletier, 2017). Importantly, disruption of F-actin leads to deficits in spindle morphology and orientation but does not alter chromosome dynamics or cell cycle timing, demonstrating that interactions with F-actin are insufficient to completely describe the Shot phenotype. Conversely, all Shot phenotypes are mimicked by loss of Arp-1, an essential component of the Dynein-activating Dynactin complex, as well as loss of Dhc itself. The ABD of Shot directly interacts with Arp-1 *in vitro*, defining a physical link with the Dynactin complex. Finally, Shot loss induces significant cell death *in vivo*, and preventing this apoptotic response leads to marked expression of MMP-1 and epithelial disorganization, both classic hallmarks of EMT. We propose that Shot, in addition to its traditional role as an actin-MT cross-linking agent, serves as an important regulator of mitotic Dynein/Dynactin activity to help ensure the fidelity and accuracy of cell division.

Shot participates in mitotic spindle assembly and orientation

The role of F-actin in mitotic spindle assembly and positioning has been studied in a variety of cellular systems (Sandquist *et al.*, 2011; Lancaster and Baum, 2014). In budding yeast, cortical actin plays an important role in centrosome guidance into the developing bud that aids in satisfying the spindle orientation checkpoint process that triggers mitotic exit (Yin *et al.*, 2000; Gachet *et al.*, 2001). A similar modality contributes to bipolar spindle formation in mammalian cells: the F-actin cortex is necessary for centrosome separation and orientation after NEB through a myosin II-dependent connection with astral MTs (Rosenblatt *et al.*, 2004). Chemical disruption of cortical actin induces spindle orientation defects in mammalian cell culture (They *et al.*, 2005; Toyoshima and Nishida, 2007). Recent studies have shown that external forces controlling cell shape can dictate spindle assembly and positioning (Fink *et al.*, 2011; Lancaster *et al.*, 2013; Petridou and Skourides, 2014). The Ezrin–Radixin–Moesin (ERM) family of proteins, which associate with the F-actin-rich cortex, represents a likely candidate for mediating this effect by ensuring cortical localization of core spindle orientation machinery (Hebert *et al.*, 2012; Kiyomitsu and Cheeseman, 2013; Machicoane *et al.*, 2014).

Arp-1 (or more generally the Dynactin complex) is also an important component of spindle assembly and positioning. Dynactin is essential for spindle orientation in *Drosophila* neural stem cells, where it is thought to exert cortical forces on spindle poles to establish proper positioning as part of a complex with Dynein and Mud/NuMA (Bowman *et al.*, 2006; Siller *et al.*, 2006; Siller and Doe, 2008). Studies in HeLa cells have shown that NuMA is necessary for asymmetric cortical Dynactin localization (including Arp-1 itself), which is critical for proper spindle positioning (Kiyomitsu and Cheeseman, 2012). In fact, this cortical localization of Dynactin is sufficient

for orienting the spindle in these cells (Kotak *et al.*, 2012). Dynactin also plays a critical role in spindle assembly, particularly in the organization of spindle poles (Merdes *et al.*, 1996, 2000; Gaglio *et al.*, 1997; Quintyne *et al.*, 1999; Morales-Mulia and Scholey, 2005).

These parallel effects of F-actin and Arp-1/Dynactin on spindle morphology and orientation complicate the interpretation of this Shot phenotype. Shot interacts with both F-actin and Arp-1, and Shot loss has effects on spindle assembly and orientation similar to those of both Cyt-D treatment and Arp-1^{RNAi}. Thus a complete molecular picture of Shot function in these processes will require further investigation. It is worth noting that Cyt-D treatment did not disrupt Shot localization in metaphasic S2 cells, a result consistent with a model in which Arp-1 plays a more important role in Shot mitotic function. Furthermore, concomitant loss of Shot and either Arp-1 or Dhc did not further potentiate the effects of either alone, suggesting they operate in a common pathway. Mitotic spindle poles represent one prominent site for Shot localization, and we suggest that Shot, a large structural protein, could physically connect cortical actin with astral MTs as a means of spindle capturing, an important and conserved feature of spindle positioning (Huisman and Segal, 2005; Johnston *et al.*, 2009). Alternatively, but not mutually exclusively, Shot interaction with Arp-1 at spindle poles could directly participate in Dynactin/Dynein activity to ensure proper focusing of MTs and the force generation created by minus-end motor activity.

Molecular model for how Shot regulates Dynein function

MT motor proteins participate in diverse cellular events. In contrast to the relatively large family of plus end-directed kinesin motor proteins, cytoplasmic Dynein represents the sole minus end-directed motor within the cell (note that at least one unique member of the kinesin family also has minus-end directionality). Yet the diversity of cellular functions involving Dynein easily matches that of the much larger kinesin superfamily. How then can this single, yet functionally diverse Dynein motor be properly regulated across its range of activities? Furthermore, Dynein/Dynactin alone is a nonprocessive motor, raising the question of how processive function can be achieved. These apparent problems are solved by the existence of a large group of “adaptor” proteins that together regulate both the localization and processive activity of the Dynein/Dynactin complex (Kardon and Vale, 2009). Dynactin itself is a large, multiprotein complex, including its core Arp-1 filament, that aids in Dynein localization, cargo assembly, and minus-end movement (Kardon and Vale, 2009). The adaptor protein BICD2 forms a tripartite complex with Dynein and Dynactin that stabilizes binding of the Dynein tail to Arp-1 (Urnavicius *et al.*, 2015). Dynactin binding induces conformational changes in the Dynein motor domains that ultimately lead to processive minus-end movements (McKenney *et al.*, 2014; Zhang *et al.*, 2017). A diverse set of these adaptor proteins may, therefore, provide spatiotemporal and functionally specific activation of Dynein activity. One such adaptor, Spindly, targets Dynein to kinetochores and is necessary for the poleward removal of the RZZ/Mad2 complex that silences SAC signaling (Griffis *et al.*, 2007). Spindly binds Dynactin; however, it associates with the Pointed-End Complex rather than the Arp-1 filament (Gama *et al.*, 2017). The ability of Shot to directly associate with the Arp-1 component of Dynactin suggests it may serve an adaptor role as well, ultimately leading to enhanced Dynein activity. Results presented herein suggest this may be particularly important in Dynein-dependent chromosome transport to spindle poles, as Shot loss leads to deficits in both chromosome congression and segregation, ultimately delaying cell cycle progression (Figures 4–6).

The mitotic arrest induced by Shot loss is phenocopied by reduction of Arp-1 or Dhc, and inhibition of the SAC by knockdown of

Rod suppresses both Shot^{RNAi}- and Arp-1^{RNAi}-mediated arrest. Interestingly, concomitant loss of Shot and Arp-1 or Shot and Dhc prevents effects on both mitotic arrest and index. Although the molecular basis for this effect is not immediately obvious, we speculate it could be due to a reduced efficiency and/or sustainability of the SAC resulting from less stable kinetochore MTs in the absence of Shot. Shot is known to function in stabilizing interphase microtubules (Applewhite *et al.*, 2010). Unstable MTs could compromise kinetochore associations; however, this would be predicted to increase SAC signaling (Tauchman *et al.*, 2015). A more plausible model could be that certain SAC components are not properly localized in the double-mutant cells, allowing anaphase transition despite chromosome congression and/or alignment errors. The MT-associated KMN network plays an important role in the recruitment of key SAC components (Varma and Salmon, 2012), the efficiency of which may be compromised in the absence of Shot. Why this effect is only seen in double RNAi (Shot/Arp-1 or Shot/Dhc) and not following Shot^{RNAi} alone remains unclear. Knockdown of both Arp-1 and Dhc does not suppress metaphase arrest, however, indicating that escape from mitotic arrest is dependent on Shot knockdown. The inability to arrest is not without consequences, as both Shot/Arp-1 and Shot/Dhc64C double RNAi-treated cells exhibited extremely high rates of chromosome segregation defects.

βIII-spectrin, a gene in the spectrin superfamily from which spectraplakins like Shot are thought to have evolved (Suozzi *et al.*, 2012), localizes to the Golgi membranes and is thought to enhance Dynein-mediated vesicle transport. Similar to Shot, βIII-spectrin interacts with Arp-1 via its N-terminal ABD, and this interaction is ablated by an L253P mutation (corresponding to Shot L340P used herein) associated with Spinocerebellar ataxia type 5, which leads to impaired vesicular transport in cerebellar axons (Holleran *et al.*, 1996, 2001; Clarkson *et al.*, 2010; Lorenzo *et al.*, 2010). In contrast to their common N-terminal ABDs, spectrins differ from spectraplakins in that they lack an MBD at the C-terminus and instead contain a phospholipid-binding pleckstrin homology (PH) domain (Suozzi *et al.*, 2012). Association of this C-terminal PH domain with acidic lipids on transport vesicles allows βIII-spectrin to thus tether cargo to the motile Dynein/Dynactin complex bound at the N-terminal ABD via Arp-1 (Johansson *et al.*, 2007). Moreover, this effect can be reconstituted *in vitro* in a manner that suggests that βIII-spectrin, through its interaction with Arp-1, is sufficient for processive Dynein-mediated vesicle transport (Muresan *et al.*, 2001). An analogous mechanism may underlie Shot aiding Dynein-mediated events during mitosis. For example, focusing of mitotic spindle poles is thought to be achieved through a multistep process, wherein processive Dynein motility allows for the transport of bundled K-fibers along centrosomal MTs (C-MTs) in a poleward direction (Goshima *et al.*, 2005). This process is thought to rely on cross-linking factors that can tether C-MT-bound Dynein/Dynactin to the K-fiber MT bundles. Shot could accomplish this through simultaneous interactions with Arp-1 at its N-terminus and K-fiber MTs at its C-terminus. This would be consistent with both the general requirement of Shot in pole focusing as well as the dependence on its intact ABDs and MBDs (Figure 4), although the precise mechanism requires further investigation.

Importance of Shot in tissue organization and possible tumor suppression

Knockdown of Shot *in vivo* results in an apoptotic response in imaginal wing disk epithelia. Interestingly, loss of Arp-1 in this tissue leads to a significantly greater level of apoptosis, demonstrating a strict requirement of this Dynactin component for epithelial cell viability. The precise mechanism by which Shot loss induces apopto-

sis is not yet elucidated, due in part to the pleiotropic mitotic errors that occur in its absence. Shot loss causes spindle misorientation in wing disks, and studies have shown that loss of planar spindle orientation leads to apoptosis of daughter cells that are basally extruded from the epithelial layer (Nakajima *et al.*, 2013). Recent studies have also shown that loss of several centrosomal proteins known to participate in spindle assembly lead to apoptosis in this tissue (Poulton *et al.*, 2014). It should be noted that centrosome loss under these conditions also leads to spindle misorientation, complicating a direct mechanistic interpretation. Thus further investigations are necessary to determine the relative contributions of defective spindle assembly and orientation in the apoptotic response seen following Shot loss. Unlike loss of other genes well known to participate in spindle assembly and orientation (Nakajima *et al.*, 2013; Poulton *et al.*, 2014), Shot loss does not appear to significantly up-regulate p-JNK levels, suggesting apoptosis is induced through an alternative pathway (Figure 7). Although JNK signaling has a clear canonical role in apoptosis, alternative pathways likely play a role in apoptotic induction (Strasser *et al.*, 2000), and furthermore, JNK signaling has been shown to play an activating role in cell proliferation under certain conditions such as compensatory growth (Mollereau and Ma, 2016).

Whatever the cause of apoptosis following Shot knockdown, results from p35 expression highlight the importance of this response in maintaining tissue architecture. Although Shot^{RNAi} expression alone results in a mild loss of organization within the wing pouch, coexpression with p35 to prevent the apoptotic response leads to a much more striking disorganization of tissue structure (Figure 7). Moreover, this genotype caused a marked induction of the EMT marker MMP-1. What the relative contributions of Shot's mitotic functions are to these defects is an important future question to resolve. Also of interest will be evaluation of the tumorigenic potential of this tissue, perhaps using recently established tumor models in *Drosophila* (Gonzalez, 2013).

MATERIALS AND METHODS

Fly stocks

The following stocks were obtained from the Bloomington Stock Center: VALIUM TRiP lines for *shot*^{RNAi} (stock # 28336), *arp-1*^{RNAi} (stock # 32032), and *sas-4*^{RNAi} (stock # 35049), as well as UAS-p35 (stock # 5072) and *nubbin*^{GAL4} (stock # 25754). The double transgenic line UAS-p35/UAS-p35;*shot*^{RNAi}/*shot*^{RNAi} was generated using a *Cyo*/Br;TM2/TM6 double balancer line (generous gift from Richard M. Cripps, University of New Mexico).

S2 cell maintenance, RNAi treatments, and transient transfection

Schneider S2 cells (Invitrogen) were grown in Schneider's insect media (Sigma) supplemented with 10% heat-inactivated fetal bovine serum (SIM). Cells were passaged every 3–4 d, and stocks were maintained at 25°C in the absence of CO₂. For transient transfections (see below), (1–2) × 10⁶ cells were placed in five-well culture dishes for 30 min in 3 ml of SIM. Cells were then transfected with 1 μg total DNA using the Effectene reagent system according to manufacturer protocols (Qiagen). Following 24–36 h incubation, transgene expression was induced by the addition of CuSO₄ (500 μM) for 24–48 h.

We used the following constructs for S2 cell transfections: Ed:GFP:Pins, Ed:GFP:Dsh, Ed:FLAG:Pins, ShotA:ACT:mCherry, and GAL4 were expressed using the copper-inducible pMT vector. ShotA:GFP and ShotC:GFP were cloned in the pUAST vector and expressed via cotransfection of pMT-GAL4. All Shot constructs, as well as the pMT-GAL4 plasmid, were generous gifts from Stephen

Rogers and Derek Applewhite (University of North Carolina, Chapel Hill and Reed College, respectively).

Primers used for RNAi construction were designed using the SnapDragon Web-based service (www.flyrnai.org/snapdragon), and all primer synthesis was carried out by Invitrogen. Primer sets that amplify segments of ~200–600 base pairs within the coding or 3'-UTR sequence of desired targets were optimized for efficiency and specificity and synthesized with T7 promoter sequence recognition tags. Targeted sequences were designed to universally recognize all possible isoforms for desired transcript. PCR-amplified target sequences were transcribed to yield double-stranded RNA using the Megascript T7 kit (Ambion) following the recommended protocol.

For RNAi treatment, S2 cells were seeded in six-well dishes at 1×10^6 cells per well in 1 ml of serum-free Schneider growth media and incubated with 10 μ g of desired RNAi. After 1 h, 2 ml of SIM was added, and cells were incubated for an additional 5 d before subsequent assays. Cells were typically supplemented with an additional 0.5–1 ml of SIM following day 3 to avoid excessive evaporation.

For the Echinoid-based "induced polarity" assay, cells were harvested, pelleted, and resuspended in fresh SIM supplemented with CuSO_4 . Cells were then placed in a new six-well dish and rotated at ~175 rpm for 2–3 h, allowing for stochastic cell collisions that lead to cell–cell contacts and cluster formation (Johnston *et al.*, 2009). Cyt-D treatments were done with 3 μ g/ml of the drug dissolved in dimethyl sulfoxide (DMSO), with an equal volume of DMSO alone serving as a vehicle control.

Immunostaining and S2 live-cell imaging

Following transfection and RNAi treatments, S2 cells were mixed with fresh SIM in 24-well dishes containing 12-mm-diameter round glass coverslips. Cells were incubated for 2–3 h to allow for adherence to coverslips and to increase the percentage of mitotic cells. Cells were then fixed using a treatment of 4% paraformaldehyde for 10 min. Fixed cells were washed three times (5 min each) with wash buffer (0.1% Triton X-100 in PBS), followed by a 1-h incubation with block buffer (0.1% Triton X-100 and 1% bovine serum albumin [BSA] in PBS). Primary antibodies diluted in block buffer were then incubated with slides overnight at 4°C. Following primary antibody incubation, slides were washed three times with block buffer. Secondary antibodies were then added and incubated at room temperature for 2 h. Antibodies were removed, and slides were washed four times with wash buffer. Finally, coverslips were inverted and mounted using EverBrite Hardset reagent (VWR) and stored at 4°C before imaging.

Antibodies used were as follows: mouse anti-FLAG (1:500; Sigma), rat anti- α -tubulin (1:500; Sigma Aldrich), and rabbit anti-phosphohistone-H3 (PH3) (1:1,000; Abcam). γ -Tubulin antibodies were obtained from Sigma (1:500, rabbit) and GeneTex (1:2,000, mouse). Imaging was performed using Nikon Eclipse Ti-S and Olympus IX83 inverted fluorescence microscopes and collected under oil immersion at 60 \times magnification. All secondary antibodies (preabsorbed and non-cross-reactive) were obtained from Jackson ImmunoResearch and used at 1:250 dilutions.

For live-cell experiments, movies (see Supplemental Movies 1–3) were acquired using S2 cells stably expressing an inducible GFP:CID (a generous gift from Gary Karpen, University of California, Berkeley), which we subsequently stably transfected with inducible mCherry- α -tubulin (selected for using puromycin resistance) to generate a stable double transgenic S2 cell line. Cells were treated with control or RNAi as described in the previous section. Upon completion of RNAi treatment, cells were settled at a density of 2 million/ml into Nunc Lab-Tek II 4-chambered coverglass chambers precoated with poly-L-lysine. After settling for 1 h, chambers were placed onto an

Olympus IX-83 inverted epifluorescence microscope, and appropriate cells were located and imaged at either 30-s or 1-min intervals using a Hamamatsu Orca-Flash 4.0LT camera, with three z-stacks taken at each interval. If cells (e.g., Shot^{RNAi} treated) did not enter anaphase after 3 h, the experiment was stopped and recorded as a 180-min data point. This was done due to significant photobleaching and the potential for phototoxicity. Movies were converted to AVI or MOV files and analyzed using ImageJ.

Protein purification

The Shot ABD (CH1+CH2 domains, aa 149–368), CH2 domain alone (aa 264–365), and C-terminus (aa 5071–5501) were PCR amplified from a pUAST-Shot construct and cloned into the pGEX vector using 5'-BamHI and 3'-XhoI restriction sites to generate GST-Shot fusion constructs. Full-length Arp-1 was PCR amplified from an S2 cell cDNA library and cloned into pBH4 using 5'-BamHI and 3'-XhoI restriction sites to generate a 6 \times His-Arp-1 fusion construct. All constructs were transformed into the BL21(DE3) strain of *E. coli* for recombinant protein expression and grown in standard Luria-Bertani broth supplemented with 100 μ g/ml ampicillin.

GST-Shot^{ABD} and GST-Shot^{CH2} were grown at 37°C to an OD₆₀₀ ~ 0.8, and protein expression was induced with 1 mM isopropyl β -D-1-thiogalactopyranoside (IPTG) for 3–4 h. GST-Shot^{CT} was grown at 30°C to an OD₆₀₀ ~ 0.6 and induced with 0.2 mM IPTG overnight at 20°C. Cells were harvested by centrifugation (5000 \times g for 10 min), and bacterial pellets were resuspended in PBS and flash-frozen in liquid nitrogen. Cells were lysed using a Branson digital sonifier and clarified by centrifugation (12,000 \times g for 30 min). Cell lysates were aliquoted and stored at –80°C until use.

His-Arp-1 expression was induced similarly to GST-Shot^{CT}, except that cells were resuspended in N1 buffer (50 mM Tris, pH 8, 500 mM NaCl, and 10 mM imidazole). Following lysis and clarification, the His-Arp-1 supernatant was incubated with nickel-NTA resin for 3 h at 4°C with constant rotation. Resin was washed extensively with both N1 buffer and wash buffer (N1 + 30 mM imidazole). Bound proteins were eluted and collected in elution buffer (20 mM Tris, pH 8, 200 mM NaCl, and 300 mM imidazole). This sample was dialyzed overnight at 4°C in buffer (20 mM Tris, pH 8, 200 mM NaCl, and 2 mM dithiothreitol [DTT]), concentrated, and stored at –80°C before use. This crude preparation produced minimal amounts of soluble His-Arp-1, although they were sufficient for detection using an anti-His antibody in Western blotting.

GST pull-down assay

Equivalent amounts of GST-fused Shot constructs were absorbed to glutathione agarose for 30 min at room temperature and washed three times with PBS to remove unbound protein. Subsequently His-Arp-1 was added for 3 h at 4°C with constant rocking in wash buffer (PBS supplemented with 0.5% Triton X-100 and 1 mM DTT). Reactions were washed four times in wash buffers, and resolved samples were analyzed by Western blot using mouse anti-His primary and bovine anti-mouse horseradish peroxidase secondary antibodies (ThermoFisher and Santa Cruz Biotechnologies).

Imaginal wing disk analysis

Imaginal wing disks were dissected from wandering third instar larvae in PBS. Disks were fixed in 4% paraformaldehyde at room temperature for 20 min with rocking. Following fixation, disks were quickly washed three times in wash buffer (PBS supplemented with 0.3% Triton X-100) and then once at room temperature for 20 min with rocking. Disks were blocked in block buffer (wash buffer supplemented with 1% BSA) for 1 h at room temperature. Phalloidin-568

(1:50, Thermo Fisher) and primary antibodies in block buffer were incubated with constant rocking at 4°C for 24–48 h. Subsequently disks were washed and treated with secondary antibodies in block buffer for 2 h at room temperature. Washed disks were mounted in Vectashield Mounting Medium for Fluorescence or 80% glycerol and stored at 4°C until imaged. Imaging was performed on a Zeiss LSM780 confocal microscope. Antibodies used were as follows: mouse γ -tubulin (1:500), rabbit phosphohistone-H3 (1:1000), rabbit cleaved caspase-3 (1:500, Cell Signaling Technology), mouse MMP-1 (1:100, Developmental Studies Hybridoma Bank), and rabbit phospho-JNK (1:1000, Promega).

Area quantification of wing disk maximum intensity projections was done using thresholding and the Threshold Colour plug-in in ImageJ. The area of the wing pouch was first taken using the polygon selection tool and recorded in pixels. The extraneous portions of the disk (the hinge and the notum that lie outside of the Nubbin expression pattern) were then removed using the Clear Outside command. Then, using the Threshold Colour command, only pixels displaying green were selected. Using the Threshold command, pixels positive for signal were selected and background was excluded. The number of positive pixels were then calculated using the Analyze Particles command, setting the minimum detectable pixel size to 2 square pixels and displaying results. The number of pixels obtained was then normalized to a percent area measurement by dividing it by the size of the wing pouch obtained earlier.

ACKNOWLEDGMENTS

We thank Johnston lab members for helpful and insightful discussions. This work was supported by a grant from the National Institutes of Health: R01-GM108756 (C.A.J.).

REFERENCES

Applewhite DA, Grode KD, Duncan MC, Rogers SL (2013). The actin-microtubule cross-linking activity of *Drosophila* Short stop is regulated by intramolecular inhibition. *Mol Biol Cell* 24, 2885–2893.

Applewhite DA, Grode KD, Keller D, Zadeh AD, Slep KC, Rogers SL (2010). The spectraplakins Short stop is an actin-microtubule cross-linker that contributes to organization of the microtubule network. *Mol Biol Cell* 21, 1714–1724.

Bader JR, Vaughan KT (2010). Dynein at the kinetochore: timing, interactions and functions. *Semin Cell Dev Biol* 21, 269–275.

Barisic M, Aguiar P, Geley S, Maiato H (2014). Kinetochore motors drive congression of peripheral polar chromosomes by overcoming random arm-ejection forces. *Nat Cell Biol* 16, 1249–1256.

Basto R, Gomes R, Karess RE (2000). Rough deal and Zw10 are required for the metaphase checkpoint in *Drosophila*. *Nat Cell Biol* 2, 939–943.

Bottenberg W, Sanchez-Soriano N, Alves-Silva J, Hahn I, Mende M, Prokop A (2009). Context-specific requirements of functional domains of the Spectraplakins Short stop in vivo. *Mech Dev* 126, 489–502.

Bowman SK, Neumuller RA, Novatchkova M, Du Q, Knoblich JA (2006). The *Drosophila* NuMA homolog Mud regulates spindle orientation in asymmetric cell division. *Dev Cell* 10, 731–742.

Cabello J, Neukomm LJ, Gunesdogan U, Burkart K, Charette SJ, Lochnit G, Hengartner MO, Schnabel R (2010). The Wnt pathway controls cell death engulfment, spindle orientation, and migration through CED-10/Rac. *PLoS Biol* 8, e1000297.

Carreno S, Kouranti I, Glusman ES, Fuller MT, Echard A, Payre F (2008). Moesin and its activating kinase Slik are required for cortical stability and microtubule organization in mitotic cells. *J Cell Biol* 180, 739–746.

Castanon I, Abrami L, Holtzer L, Heisenberg CP, van der Goot FG, Gonzalez-Gaitan M (2012). Anthrax toxin receptor 2a controls mitotic spindle positioning. *Nat Cell Biol* 15, 28–39.

Clarkson YL, Gillespie T, Perkins EM, Lyndon AR, Jackson M (2010). Beta-III spectrin mutation L253P associated with spinocerebellar ataxia type 5 interferes with binding to Arp1 and protein trafficking from the Golgi. *Hum Mol Genet* 19, 3634–3641.

Dewey EB, Sanchez D, Johnston CA (2015). Warts phosphorylates Mud to promote Pins-mediated mitotic spindle orientation in *Drosophila*, independent of Yorkie. *Curr Biol* 25, 2751–2762.

Fink J, Carpi N, Betz T, Betard A, Chebah M, Azioune A, Bornens M, Sykes C, Fetler L, Cuvelier D, et al. (2011). External forces control mitotic spindle positioning. *Nat Cell Biol* 13, 771–778.

Fletcher DA, Mullins RD (2010). Cell mechanics and the cytoskeleton. *Nature* 463, 485–492.

Gachet Y, Tournier S, Millar JB, Hyams JS (2001). A MAP kinase-dependent actin checkpoint ensures proper spindle orientation in fission yeast. *Nature* 412, 352–355.

Gaglio T, Dionne MA, Compton DA (1997). Mitotic spindle poles are organized by structural and motor proteins in addition to centrosomes. *J Cell Biol* 138, 1055–1066.

Gaglio T, Saredi A, Bingham JB, Hasbani MJ, Gill SR, Schroer TA, Compton DA (1996). Opposing motor activities are required for the organization of the mammalian mitotic spindle pole. *J Cell Biol* 135, 399–414.

Gama JB, Pereira C, Simoes PA, Celestino R, Reis RM, Barbosa DJ, Pires HR, Carvalho C, Amorim J, Carvalho AX, et al. (2017). Molecular mechanism of dynein recruitment to kinetochores by the Rod-Zw10-Zwlich complex and Spindly. *J Cell Biol*, doi: 10.1083/jcb.201610108.

Glotzer M (2005). The molecular requirements for cytokinesis. *Science* 307, 1735–1739.

Gonzalez C (2013). *Drosophila melanogaster*: a model and a tool to investigate malignancy and identify new therapeutics. *Nat Rev Cancer* 13, 172–183.

Goshima G, Nedelec F, Vale RD (2005). Mechanisms for focusing mitotic spindle poles by minus end-directed motor proteins. *J Cell Biol* 171, 229–240.

Griffis ER, Stuurman N, Vale RD (2007). Spindly, a novel protein essential for silencing the spindle assembly checkpoint, recruits dynein to the kinetochore. *J Cell Biol* 177, 1005–1015.

Hariharan IK (2015). Organ size control: lessons from *Drosophila*. *Dev Cell* 34, 255–265.

Heald R, Tournebise R, Blank T, Sandaltzopoulos R, Becker P, Hyman A, Karsenti E (1996). Self-organization of microtubules into bipolar spindles around artificial chromosomes in *Xenopus* egg extracts. *Nature* 382, 420–425.

Hebert AM, DuBoff B, Casaletto JB, Gladden AB, McClatchey AI (2012). Merlin/ERM proteins establish cortical asymmetry and centrosome position. *Genes Dev* 26, 2709–2723.

Holleran EA, Ligon LA, Tokito M, Stankewich MC, Morrow JS, Holzbaur EL (2001). Beta III spectrin binds to the Arp1 subunit of dynactin. *J Biol Chem* 276, 36598–36605.

Holleran EA, Tokito MK, Karki S, Holzbaur EL (1996). Centractin (ARP1) associates with spectrin revealing a potential mechanism to link dynactin to intracellular organelles. *J Cell Biol* 135, 1815–1829.

Howell BJ, McEwen BF, Canman JC, Hoffman DB, Farrar EM, Rieder CL, Salmon ED (2001). Cytoplasmic dynein/dynactin drives kinetochore protein transport to the spindle poles and has a role in mitotic spindle checkpoint inactivation. *J Cell Biol* 155, 1159–1172.

Huber F, Boire A, Lopez MP, Koenderink GH (2015). Cytoskeletal crosstalk: when three different personalities team up. *Curr Opin Cell Biol* 32, 39–47.

Huisman SM, Segal M (2005). Cortical capture of microtubules and spindle polarity in budding yeast—where’s the catch? *J Cell Sci* 118, 463–471.

Ikeda Y, Dick KA, Weatherspoon MR, Gincel D, Armbrust KR, Dalton JC, Stevanin G, Durr A, Zuhlke C, Burk K, et al. (2006). Spectrin mutations cause spinocerebellar ataxia type 5. *Nat Genet* 38, 184–190.

Johansson M, Rocha N, Zwart W, Jordens I, Janssen L, Kuijl C, Olkkonen VM, Neefjes J (2007). Activation of endosomal dynein motors by stepwise assembly of Rab7-RILP-p150Glued, ORP1L, and the receptor betalll spectrin. *J Cell Biol* 176, 459–471.

Johnston CA, Hirono K, Prehoda KE, Doe CQ (2009). Identification of an Aurora-A/Pins/LINKER/Dlg spindle orientation pathway using induced cell polarity in S2 cells. *Cell* 138, 1150–1163.

Johnston CA, Manning L, Lu MS, Golub O, Doe CQ, Prehoda KE (2013). Formin-mediated actin polymerization cooperates with Mushroom body defect (Mud)-Dynein during Frizzled-Dishevelled spindle orientation. *J Cell Sci* 126, 4436–4444.

Kardon JR, Vale RD (2009). Regulators of the cytoplasmic dynein motor. *Nat Rev Mol Cell Biol* 10, 854–865.

Khanal I, Elbediwy A, Diaz de la Loza Mdel C, Fletcher GC, Thompson BJ (2016). Shot and Patronin polarise microtubules to direct membrane traffic and biogenesis of microvilli in epithelia. *J Cell Sci* 129, 2651–2659.

Kim Y, Holland AJ, Lan W, Cleveland DW (2010). Aurora kinases and protein phosphatase 1 mediate chromosome congression through regulation of CENP-E. *Cell* 142, 444–455.

Kiyomitsu T, Cheeseman IM (2012). Chromosome- and spindle-pole-derived signals generate an intrinsic code for spindle position and orientation. *Nat Cell Biol* 14, 311–317.

- Kiyomitsu T, Cheeseman IM (2013). Cortical dynein and asymmetric membrane elongation coordinately position the spindle in anaphase. *Cell* 154, 391–402.
- Kodama A, Karakesisoglou I, Wong E, Vaezi A, Fuchs E (2003). ACF7: an essential integrator of microtubule dynamics. *Cell* 115, 343–354.
- Kotak S, Busso C, Gonczy P (2012). Cortical dynein is critical for proper spindle positioning in human cells. *J Cell Biol* 199, 97–110.
- Kunda P, Baum B (2009). The actin cytoskeleton in spindle assembly and positioning. *Trends Cell Biol* 19, 174–179.
- Kunda P, Pelling AE, Liu T, Baum B (2008). Moesin controls cortical rigidity, cell rounding, and spindle morphogenesis during mitosis. *Curr Biol* 18, 91–101.
- Lancaster OM, Baum B (2014). Shaping up to divide: coordinating actin and microtubule cytoskeletal remodelling during mitosis. *Semin Cell Dev Biol* 34, 109–115.
- Lancaster OM, Le Berre M, Dimitracopoulos A, Bonazzi D, Zlotek-Zlotkiewicz E, Picone R, Duke T, Piel M, Baum B (2013). Mitotic rounding alters cell geometry to ensure efficient bipolar spindle formation. *Dev Cell* 25, 270–283.
- Lee S, Kolodziej PA (2002). Short Stop provides an essential link between F-actin and microtubules during axon extension. *Development* 129, 1195–1204.
- Levine BA, Moir AJ, Patchell VB, Perry SV (1992). Binding sites involved in the interaction of actin with the N-terminal region of dystrophin. *FEBS Lett* 298, 44–48.
- Li R, Gundersen GG (2008). Beyond polymer polarity: how the cytoskeleton builds a polarized cell. *Nat Rev Mol Cell Biol* 9, 860–873.
- Lorenzo DN, Li MG, Mische SE, Armbrust KR, Ranum LP, Hays TS (2010). Spectrin mutations that cause spinocerebellar ataxia type 5 impair axonal transport and induce neurodegeneration in *Drosophila*. *J Cell Biol* 189, 143–158.
- Lu MS, Johnston CA (2013). Molecular pathways regulating mitotic spindle orientation in animal cells. *Development* 140, 1843–1856.
- Machicoane M, de Frutos CA, Fink J, Rocancourt M, Lombardi Y, Garel S, Piel M, Echard A (2014). SLK-dependent activation of ERMs controls LGN-NuMA localization and spindle orientation. *J Cell Biol* 205, 791–799.
- Maiato H, Rieder CL, Khodjakov A (2004). Kinetochore-driven formation of kinetochore fibers contributes to spindle assembly during animal mitosis. *J Cell Biol* 167, 831–840.
- McKenney RJ, Huynh W, Tanenbaum ME, Bhabha G, Vale RD (2014). Activation of cytoplasmic dynein motility by dynactin-cargo adapter complexes. *Science* 345, 337–341.
- Merdes A, Heald R, Samejima K, Earnshaw WC, Cleveland DW (2000). Formation of spindle poles by dynein/dynactin-dependent transport of NuMA. *J Cell Biol* 149, 851–862.
- Merdes A, Ramyar K, Vechio JD, Cleveland DW (1996). A complex of NuMA and cytoplasmic dynein is essential for mitotic spindle assembly. *Cell* 87, 447–458.
- Mollereau B, Ma D (2016). Rb-mediated apoptosis or proliferation: it's up to JNK. *Cell Cycle* 15, 11–12.
- Morales-Mulia S, Scholey JM (2005). Spindle pole organization in *Drosophila* S2 cells by dynein, abnormal spindle protein (Asp), and KLP10A. *Mol Biol Cell* 16, 3176–3186.
- Moulding DA, Blundell MP, Spiller DG, White MR, Cory GO, Calle Y, Kempski H, Sinclair J, Ancliff PJ, Kinnon C, et al. (2007). Unregulated actin polymerization by WASp causes defects of mitosis and cytokinesis in X-linked neutropenia. *J Exp Med* 204, 2213–2224.
- Mui UN, Lubczyk CM, Nam SC (2011). Role of spectraplakins in *Drosophila* photoreceptor morphogenesis. *PLoS One* 6, e25965.
- Muresan V, Stankewich MC, Steffen W, Morrow JS, Holzbaur EL, Schnapp BJ (2001). Dynactin-dependent, dynein-driven vesicle transport in the absence of membrane proteins: a role for spectrin and acidic phospholipids. *Mol Cell* 7, 173–183.
- Nakajima Y, Meyer EJ, Kroesen A, McKinney SA, Gibson MC (2013). Epithelial junctions maintain tissue architecture by directing planar spindle orientation. *Nature* 500, 359–362.
- Nashchekin D, Fernandes AR, St Johnston D (2016). Patronin/Shot cortical foci assemble the noncentrosomal microtubule array that specifies the *Drosophila* anterior-posterior axis. *Dev Cell* 38, 61–72.
- Nestor-Bergmann A, Goddard G, Woolner S (2014). Force and the spindle: mechanical cues in mitotic spindle orientation. *Semin Cell Dev Biol* 34, 133–139.
- Ning W, Yu Y, Xu H, Liu X, Wang D, Wang J, Wang Y, Meng W (2016). The CAMSAP3-ACF7 complex couples noncentrosomal microtubules with actin filaments to coordinate their dynamics. *Dev Cell* 39, 61–74.
- Petridou NI, Skourides PA (2014). FAK transduces extracellular forces that orient the mitotic spindle and control tissue morphogenesis. *Nat Commun* 5, 5240.
- Poulton JS, Cunningham JC, Peifer M (2014). Acentrosomal *Drosophila* epithelial cells exhibit abnormal cell division, leading to cell death and compensatory proliferation. *Dev Cell* 30, 731–745.
- Prokop A, Uhler J, Roote J, Bate M (1998). The kakapo mutation affects terminal arborization and central dendritic sprouting of *Drosophila* motoneurons. *J Cell Biol* 143, 1283–1294.
- Prosser SL, Pelletier L (2017). Mitotic spindle assembly in animal cells: a fine balancing act. *Nat Rev Mol Cell Biol* 18, 187–201.
- Quintyne NJ, Gill SR, Eckley DM, Crego CL, Compton DA, Schroer TA (1999). Dynactin is required for microtubule anchoring at centrosomes. *J Cell Biol* 147, 321–334.
- Raaijmakers JA, Tanenbaum ME, Medema RH (2013). Systematic dissection of dynein regulators in mitosis. *J Cell Biol* 201, 201–215.
- Ramkumar N, Baum B (2016). Coupling changes in cell shape to chromosome segregation. *Nat Rev Mol Cell Biol* 17, 511–521.
- Rosenblatt J, Cramer LP, Baum B, McGee KM (2004). Myosin II-dependent cortical movement is required for centrosome separation and positioning during mitotic spindle assembly. *Cell* 117, 361–372.
- Sabino D, Gogendeau D, Gambarotto D, Nano M, Penetier C, Dingli F, Arras G, Loew D, Basto R (2015). Moesin is a major regulator of centrosome behavior in epithelial cells with extra centrosomes. *Curr Biol* 25, 879–889.
- Sanchez-Soriano N, Travis M, Dajas-Bailador F, Goncalves-Pimentel C, Whitmarsh AJ, Prokop A (2009). Mouse ACF7 and *drosophila* short stop modulate filopodia formation and microtubule organization during neuronal growth. *J Cell Sci* 122, 2534–2542.
- Sandquist JC, Kita AM, Bement WM (2011). And the dead shall rise: actin and myosin return to the spindle. *Dev Cell* 21, 410–419.
- Sawin KE, LeGuellec K, Philippe M, Mitchison TJ (1992). Mitotic spindle organization by a plus-end-directed microtubule motor. *Nature* 359, 540–543.
- Sharp DJ, Rogers GC, Scholey JM (2000). Cytoplasmic dynein is required for poleward chromosome movement during mitosis in *Drosophila* embryos. *Nat Cell Biol* 2, 922–930.
- Siller KH, Cabernard C, Doe CQ (2006). The NuMA-related Mud protein binds Pins and regulates spindle orientation in *Drosophila* neuroblasts. *Nat Cell Biol* 8, 594–600.
- Siller KH, Doe CQ (2008). Lis1/dynactin regulates metaphase spindle orientation in *Drosophila* neuroblasts. *Dev Biol* 319, 1–9.
- Siller KH, Serr M, Steward R, Hays TS, Doe CQ (2005). Live imaging of *Drosophila* brain neuroblasts reveals a role for Lis1/dynactin in spindle assembly and mitotic checkpoint control. *Mol Biol Cell* 16, 5127–5140.
- Strasser A, O'Connor L, Dixit VM (2000). Apoptosis signaling. *Annu Rev Biochem* 69, 217–245.
- Suozzi KC, Wu X, Fuchs E (2012). Spectraplakins: master orchestrators of cytoskeletal dynamics. *J Cell Biol* 197, 465–475.
- Tauchman EC, Boehm FJ, DeLuca JG (2015). Stable kinetochore-microtubule attachment is sufficient to silence the spindle assembly checkpoint in human cells. *Nat Commun* 6, 10036.
- They M, Racine V, Pepin A, Piel M, Chen Y, Sibarita JB, Bornens M (2005). The extracellular matrix guides the orientation of the cell division axis. *Nat Cell Biol* 7, 947–953.
- Toyoshima F, Nishida E (2007). Integrin-mediated adhesion orients the spindle parallel to the substratum in an EB1- and myosin X-dependent manner. *EMBO J* 26, 1487–1498.
- Urnavicius L, Zhang K, Diamant AG, Motz C, Schlager MA, Yu M, Patel NA, Robinson CV, Carter AP (2015). The structure of the dynactin complex and its interaction with dynein. *Science* 347, 1441–1446.
- Varma D, Salmon ED (2012). The KMN protein network—chief conductors of the kinetochore orchestra. *J Cell Sci* 125, 5927–5936.
- Walczak CE, Vernos I, Mitchison TJ, Karsenti E, Heald R (1998). A model for the proposed roles of different microtubule-based motor proteins in establishing spindle bipolarity. *Curr Biol* 8, 903–913.
- Wu X, Kodama A, Fuchs E (2008). ACF7 regulates cytoskeletal-focal adhesion dynamics and migration and has ATPase activity. *Cell* 135, 137–148.
- Yang Z, Tulu US, Wadsworth P, Rieder CL (2007). Kinetochore dynein is required for chromosome motion and congression independent of the spindle checkpoint. *Curr Biol* 17, 973–980.
- Yin H, Pruyne D, Huffaker TC, Bretscher A (2000). Myosin V orientates the mitotic spindle in yeast. *Nature* 406, 1013–1015.
- Zhang K, Foster HE, Rondelet A, Lacey SE, Bahi-Buisson N, Bird AW, Carter AP (2017). Cryo-EM reveals how human cytoplasmic dynein is auto-inhibited and activated. *Cell* 169, 1303–1314.